Space and Energy Distribution of Dark Matter

Åsmund Blitzner

Department of Physics and Technology

University of Bergen

A thesis submitted for the degree of

Master's Thesis in Theoretical Particle Physics

November 2011

Abstract

I start by an introduction to the notion of, and motivation for, Dark Matter, as well as a short motivation for supersymmetry, the theoretical framework usually examined when looking for places that dark matter may hide. After assuming a gravitino undergoing $\tilde{g} \to \nu\gamma$ decay, as a matter of convenience, there follows an exposition and use of the necessary tools to calculate the flux one might expect from galactic and extragalactic sources under such circumstances. The galactic model choice is given only a cursory glance, in anticipation of its ultimately minor importance to my main goal. That is, to determine if the decay of gravitinos over cosmological timescales is something that could influence our signal for reasonable values of the mean life.

Acknowledgements

When something is in the works for as long as this thesis has been, it follows that there are a lot of people who have influenced and helped me along the way, and who deserve my warm thanks. By necessity I will limit myself. Let me start with Per Osland, my supervisor. On hand with lucid, patient explanations, and exactly the right amount of follow up. Next there is my closest family, an inexhaustible source of support and encouragement, you mean the world to me. As do my friends. There are so many, and enough time has passed that some of you have weaved in and out of my life throughout the process, helping me shoulder the burden when I needed you. I love you all to bits. None of you are forgotten, but with such a huge and proud list, I will only name one. Ingelinn, for being my friend through all of this, for your stellar humour, your infallible knack for twisting my perspective to where I need it to be, and your absolutely glorious cabin trips. Thank you.

Thank you all.

Contents

List of Figures

Chapter 1

Introduction

1.1 The Standard Model

Presently, the most successful model we have of the physical world is called "The Standard Model". This model paints a world that can be interpreted as consisting of omnipresent quantum fields, the excitations of which are percieved as particles. The fields are divided into two classes. Excitations of fermion and boson-fields represent (roughly) the particles of matter, and the particles mediating the forces acting between those particles of matter, respectively. Electrons are a well known and ubiquitous example of a fermionic particle. When moving relative to each other, electrons experience an electromagnetic force, as mediated by the bosonic photons [1, 2].

So The Standard Model deals with a small handful of different forces and their mediating particles. In addition there is a rather larger zoo of particles affected by these forces. Let's list the forces, along with their force carriers and some places they pop up in everyday existence: The strong force, mediated by gluons and responsible for binding quarks into nucleons, as well as nucleons into nuclei; the weak force, mediated by W^+, W^- and Z^0 particles, is mainly known for its role in radioactive beta decay; the electromagnetic force, mediated by photons and the reason for just about everything else, with the exception of gravity. That there is no accepted theory of quantum gravity is widely regarded as perhaps the single biggest obstacle in the search for a "Theory Of Everything" that can incorporate all our knowledge in one comprehensive framework [3].

One of the most stunning successes of the Standard Model is the unification of the weak and the electromagnetic force into a single *electroweak* force at high energies. Although the weak and electromagnetic forces seem disparate at the energy levels where we most often see them, at energies north of about 100 GeV they reveal themselves to be merely different manifestations of what is, at this level, a single force.

Central to the electroweak theory is something called the Higgs mechanism, which is how particles are thought to attain their mass. If this approach is correct, we should be able to find the particle credited with making the universe massive: The Higgs particle. Vast amounts of manpower and equipment is currently being directed towards the search for the Higgs particle. If this search ultimately turns up nothing, the Standard Model is arguably in deep trouble. Nevertheless, in light of all its other successes, the scientific community remains optimistic.

Many of the particles in the Standard Model have a one-to-one correspondence with a field: An electron is an excitation of the electron field. But there are also examples of particles that are linear combinations of fields. While the electroweak force is mediated by photons, $W^{\pm}$ and Z^0 bosons, you can not point to a Z^0-field that is strictly analogous to the electron-field. Instead, we deal with $W^{\pm}, W^0$ and B^0-fields. The photon and Z-particle turn up as linear combinations of the B^0 and W^0-fields. For the benefit of the three laymen who may or may not read this: When something is a linear combination, it simply means that it behaves in a certain fairly transparent way mathematically.

Sadly (or happily, depending on your perspective), our current picture is not without its problems. Already mentioned is the fact that we haven't actually *found* the Higgs particle yet, or the ever-elusive theory of quantum gravity. Another example is the *hierarchy problem*. That is, why is gravity so laughably weak compared to the other fundamental forces [4]? These are all interesting problems, subject of much serious research and intense back-of-envelope doodles. But it is another problem that will be the focus of this thesis. There is something close to consensus that when we raise our eyes to marvel at the rest of the universe, we see maybe 20% of what is there. The remaining 80% is missing. And there seems to be no viable candidates among the particles of the Standard Model to make up this missing mass.

1.2 Dark Matter

In his paper "Die Rotverschiebung von Extragalaktischen Nebeln"(1933) [5] Fritz Zwicky became the first person to infer the existence of cosmologically significant quantities of non-luminous matter in the universe [6]. Specifically, in Zwicky's case, its presence in the Coma cluster. A cluster of galaxies some 320 million light years away just off the north galactic pole and comprised of thousands of galaxies, the Coma cluster is one of the densest clusters we know of. In his paper, and the following "On the Masses of Nebulae and of Clusters of Nebulae", Zwicky showed that the previously used methods of calculating the masses of nebulae based on their luminosities and internal rotations could only be relied upon to calculate lower limits of mass [7]. Using the virial theorem from classical mechanics, Zwicky found that the speed at which the nebulae moved implied a mass 400 times greater than what was accounted for by luminous mass.

When you're working in the field of cosmology, the knowledge that the universe is expanding at an ever-increasing rate, and that distant galaxies remove themselves from our company with more gusto than our closer neighbours, will be of some importance more often than not. To describe exactly how much faster distant galaxies recede, we use the Hubble paramater. It was named after the American astronomer Edwin Hubble, who is credited with bringing to the attention of humanity that we needed the parameter in the first place. Current estimates put it at about $H_0 = 73$ km/(s Mpc). Zwicky used a Hubble parameter $H_0 = 558$ km/(s Mpc), and the estimate therefore needs to be adjusted from 400 to 50 [8], but his point still stands. All constants and parameters, like for instance H_0 are found in [9], and I've also listed them in appendix A.

This notion of missing mass did not find traction right away, but more evidence was found, studying several different phenomena, and by 1975 a majority of astronomers were convinced that missing mass existed in significant quantities [8], although a lot of this missing mass' exact nature remained a mystery. Hot gas, brown dwarves, black holes, what? What follows is a brief summary of some of the most compelling evidence in favor of the existence of non-electromagnetically interacting, i.e. dark, matter. Please note that opponents of Dark Matter theory hold that most of these examples could potentially also be explained by a change in our theory of gravity, such as MOND [10]. This possibility will be handled separately at a later stage.

1.2.1 Evidence of Dark matter

Similarly to Zwicky's observations of velocities in galaxy clusters, studies of the rotational velocities in galaxies do not reveal anything close to a Keplerian drop-off. This is what one would expect if the mass of the galaxy was concentrated in its luminous centre. Vera Rubin and W. Kent Ford Jr. published the first result demonstrating this phenomenon for the Andromeda nebula in 1970 [11]. Over the next years they studied a slew of galaxies of various types, and papers in -80 and -85 covering 21 and 54 galaxies, respectively, drive the point home [12]. The rotational curve sketched in figure 1.1 would not be observed if, in

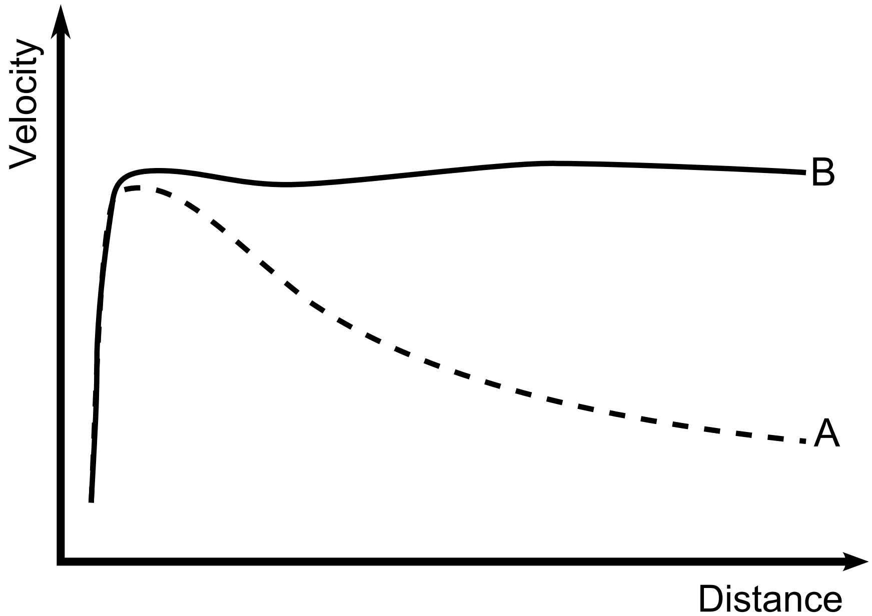

Figure 1.1: A qualitative representation of galactic rotational curves. The dashed line, A, shows the Keplerian drop-off expected from luminous matter alone. The solid line, B, is indicative of the behavior found empirically [13].

the context of matter, what you saw was what you got. The flattening out of the curve as distance increases implies that the mass of the galaxy increases linearly for large **r**. Rubin's calculations show that ordinary matter can account for only 10% of the mass needed.

To obtain the mass of a galaxy cluster by way of the virial theorem, or the rotational curve of a galaxy via spectroscopy, you need to make a few assumptions concerning the dynamics of the system. To get indications of dark matter by an independent method, scientists have used The General Theory of Relativity's prediction that the force of gravity bends the path of light [14]. This means that astronomical objects such as stars, galaxies or galaxy clusters can be used as lenses to facilitate the study of other faraway objects. But you can also flip this around: By studying the manner in which the geometry of these faraway objects is distorted before reaching us, we may deduce properties of our gravitational lens, e.g. its gravitational potential and by extension its mass distribution. Zwicky pointed this out in 1937. This is analogous to how our image in a funhouse mirror leads us to the conclusion that the mirror itself is not quite kosher. Measurements by way of gravitational lensing match up nicely with measurements done by other methods [15]. Gravitational lensing has the advantage that its result does not depend on any assumptions made concerning dynamics [16].

Our next indication that something strange and beautiful is going on, the observations of the collision taking place in the Bullet Cluster as published by Clowe et al. [17] differ from the other examples in a very important way: In this case the gravitational lensing reveals that the gravitational potential does not coincide with the distribution of visible baryonic matter. As the collision unfolds, the galaxies, interacting gravitationally, pass through to either side relatively unhindered. However *"...the fluid-like X-ray emitting intracluster plasma experiences ram pressure. Therefore, in the course of a cluster collision, galaxies spatially decouple from the plasma."* [17].

Ram pressure is the force experienced by an object as it moves through a fluid. In this case, that means the force exerted by the intracluster plasma of the respective clusters as the plasmas attempt to move through each other. This slows the plasma down to a far greater extent than the much denser galaxies, resulting in the galaxies ending up on either side, spatially decoupled from the plasma in the middle.

As the lion's share of luminous matter in the cluster, as far as we know, consists of this plasma, one would expect the gravitational potential to reflect this, if there is no dark matter to be found. However, gravitational lensing indicate large amounts of matter that has, like the stars, passed through the collision to either side of the merging cluster. This is taken to be gravitationally interacting dark matter that has been spatially decoupled from most of the luminous matter in the system. Since it doesn't interact electromagnetically, it doesn't experience ram pressure. Proponents of DM-theory hold this as an example of something that is hard, if not impossible, to explain through a modification of the theory of gravity alone.

As a final example, dark matter is also necessary in the current mainstream cosmological model in order to explain the large scale structure of the universe. Without dark matter, there would simply not be enough time since the radiation matter decoupling for the normal baryonic matter to form the galaxies, and clusters of galaxies, that we see today. However, since dark matter does not interact electromagnetically, it would be able to form gravitationally bound structures much sooner, getting a head start. Starting as primordial fluctuations, and coalescing into progressively bigger structures, dark matter provides a framework that is all ready by the time of decoupling for the baryonic mass to "fall into". This head start then, allows enough time for the observed structures of our universe to be formed [18].

1.2.2 Alternatives to Dark Matter – MOND

We have not yet found any particle that will fullfil the role of dark matter. The evidence that has us looking for it anyway is, with the possible exception of the Bullet Cluster, largely indirect. This is especially clear in the case of galaxy rotational curves and the speed of galaxies in clusters. Looking at a galaxy, one observes that the stars move faster than they "should". More mass is needed to keep them in place. But there could be another way: What if it turns out that it is our notion of gravity that is wrong? A new theory of gravity could conceivably explain the dynamics of galaxies and galaxy clusters in terms of the baryonic matter we already know is there. Modified Newtonian Dynamics (MOND) is the name of what is arguably the most popular and well-known of these theories. Mordehai Milgrom proposed the theory in 1983 [10, 19], as an alternative to dark matter.

The basic assumption of MOND is that Newton's theory of gravity fails for very weak potentials. The true gravitational attraction (acceleration) is seen as being related to its Newtonian counterpart by [20]:

$$\mathbf{g}\mu\left(\frac{|g|}{a_0}\right) = \mathbf{g_n} = \frac{GM}{r^2}\hat{\mathbf{r}}$$

where a bold font indicates a vector, $a_0 \approx 10^{-8}$ km/s^2 is a natural constant, $\hat{\mathbf{r}}$ is a unit vector in the direction of separation between the mass M and whatever it's working upon, and μ is a scalar function with $|g|/a_0$ as its argument. The exact behaviour of μ need not be known. What is important is its asymptotic behaviour:

$$\mu \simeq \begin{cases} \frac{|g|}{a_0}, & \frac{|g|}{a_0} \ll 1 \\ 1, & \frac{|g|}{a_0} \gg 1 \end{cases} \tag{1.1}$$

Now, what happens for weak gravity?

$$\mathbf{g}\mu\left(\frac{|g|}{a_0}\right) = \frac{g^2}{a_0}\hat{\mathbf{r}} = \mathbf{g_n} = \frac{GM}{r^2}\hat{\mathbf{r}}$$

$$g = \frac{\sqrt{GMa_0}}{r} = a_c = \frac{v^2}{r}$$

$$v^4 = GMa_0$$

We see that the rotational speed, v, is independent of the distance, r, which gives a flat rotational curve.

MOND has had notable success in describing galactic rotational curves. More so than the dark matter paradigm [21]. However, dark matter is considered superior to MOND by many in its treatment of many other areas: Large scale structure and behaviour in the universe, anything larger than a single galaxy in particular; anisotropies in the Cosmic Microwave Background radiation; and the gravitational potential of the Bullet Cluster. Because of this, the majority of scientists are convinced of the existence of dark matter, and that any future theories of cosmology will reflect this.

1.2.3 Candidates for Dark Matter

A viable dark matter candidate needs to satisfy a list of demands. First of all, it must by definition not interact electromagnetically (Well, mostly. Some recent papers suggest that there could be higher order electroweak corrections to the annihilation process. This could be noticed in the traces you look for when searching for it indirectly [22]). It can not be massless. Weak interaction is generally considered a virtue, as it is the sole remaining feature that can make a candidate directly detectable. Candidates for dark matter that are weakly interacting fall in a class called Weakly Interacting Massive Particles (WIMPs). We have some further demands: In light of the fact that our current explanation of the early development of large scale structure depends upon dark matter, it must have been there since the very beginning, in amounts sufficient to do what we need it to. For WIMPs, it is a popular theory that the Big Bang produced all the dark matter we need, and that it has avoided self- annihilation until now. Either through an initial slight asymmetry similar to the one we think explain why there is so much matter and so little antimatter in the universe, or through thermal freeze-out. That is, as the universe cools and expands, eventually there are few enough WIMPs around that they cease to self-interact [6].

The Standard Model seems to already provide a suitable candidate to make up these particles. Neutrinos, being stable and weakly interacting, seem promising. However, constraints on the standard model leads to the conclusion that only a fraction of the dark matter could possibly consist of neutrinos. Furthermore, these neutrinos would be hot, i.e. move at relativistic speeds, and hot dark matter is inconsistent with our current understanding of the formation of structure in our universe.

Looking beyond the standard model, several possibilities are suggested by a supersymmetric extension of the same. Indeed, since supersymmetric theory has a lot of free parameters, the possible range of candidate characteristics is larger than one might hope for. Supersymmetry posits that every particle has a superpartner (sparticles) with a spin that differs by one half. That means the superpartner of a boson would be a fermion, and vice versa. Since no sparticles have been observed, it follows that if supersymmetry is a reality, the superpartners must nevertheless have different masses from their standard model counterparts. In other words, supersymmetry must be *broken*.

Bearing dark matter in mind, models that conserve R-parity are interesting. R-parity is defined as $R = (-1)^{3B+L+2S}$, where B, L and S are the baryon number, lepton number and spin, respectively. It follows that $R = +1$ for particles, and $R = -1$ for all sparticles. Conservation of R-parity then, means that the lightest supersymmetric particle (LSP) cannot decay, and is stable over cosmological timescales. The exact identity of the LSP depends on how supersymmetry is broken, but a viable dark matter candidate needs to be colorless as well as electromagnetically neutral [23], which leaves a fairly short list of supersymmetric suspects:

- Neutralinos
  The superpartners of the B, W_3, H_1^0 and H_2^0 bosons (SUSY-models need multiple Higgs bosons) mix into four mass eigenstates called *neutralinos*. The lightest of these, often called simply *the neutralino*, is an extremely popular candidate for dark matter.

- Sneutrinos
  The spartners of standard-model neutrinos are WIMPs. However, this particular candidate opens up for direct detection experiments that have ruled out this possibility [6].

- Gravitinos
  Assuming that R-parity is conserved, the gravitino has the unwelcome distinction of being impossible to detect in many SUSY models. But if R-parity is only slightly broken, the gravitino might still be present in a cosmologically significant amount, while every so often decaying into something we can observe.

Recently, there are also people looking into the idea that the observed structure of the universe on a smaller scale has a better fit with simulation data if one supposes dark matter to be warm. As the term suggests, this means it has a higher mean velocity than the hypothesized cold dark matter, but it's still not relativistc. See for example [24], where they compare the properties of the Milky Way's surrounding dwarf galaxies with that of simulations based on both cold and warm dark matter. I will stick to the relatively more well known waters of a CDM made up of gravitinos.

Chapter 2

Revisiting the Standard Model

2.1 A motivation for SUSY

The purpose of this chapter is to outline briefly the progress from the theory of Quantum Mechanics, by way of Quantum Field Theory, to that of Supersymmetry, so that we may appreciate to some extent a motivation for imposing something as strange as SUSY on our theories. The notion of imposing symmetry is not something that is unique to SUSY, conjured up to provide us with much needed dark matter particles. Rather, demanding our theories to obey symmetries routinely reveals essential mechanisms at play in our world.

2.2 Quantum Field Theory

The first steps from ordinary Quantum Mechanics, by all accounts a tremendously successful model in its own right, to the Standard Model was motivated by a desire to make QM work at relativistic speeds [2].

The Schrödinger Equation, perhaps the most famous equation of Quantum Mechanics, describes the evolution of a physical system over time, but flounders when asked to handle the appearing and disappearing of particles within that system. At relativistic speeds, particles carry enough energy to bring the phenomenally famous equation $E = mc^2$ into play. Particles may abruptly 'pop out of existence', to be instantly replaced by different ones. Entities normally associated with matter may even be replaced by something we think of as a force carrier. After the Theory of Quantum Mechanics formalized the notion that particles can exhibit wavelike behaviour, and vice versa, these identity changes at high energies further contribute to weaken the already shaky barriers between matter and force.

In Quantum Mechanics, the Schrödinger equation is a complete description of the system. For this new framework, that role is taken by the *Lagrangian Density*, $\mathcal{L}$.

Classically, the Lagrangian is equal to the kinetic minus the potential energy of a system, and lets us define the system's *action*, S. For a particle moving in one dimension, the action is:

$$S = \int_0^t L(x, \dot{x})\mathrm{d}t$$

So to get the action, we integrate the Lagrangian over all points along the path of the particle from x_1 to x_2. The Hamiltonian, which is so important in the study of the behaviour of a system can be expressed in terms of the Lagrangian,

$$H = \dot{x}p - L$$

where p is the canonical momentum, defined by

$$p = \frac{\partial \mathcal{L}}{\partial \dot{x}}$$

Describing a system of n particles turns the equations into sums in the obvious manner.

$$L_i = L(x_i, \dot{x}_i)$$

$$S = \sum_{i=0}^{n} \int_0^t L_i \mathrm{d}t$$

$$H = \sum_{i=0}^{n} H_i = \sum_{i=0}^{n} \dot{x}_i p_i - L_i$$

It turns out that it is convenient to express the system in terms of a set of generalized coordinates: These are linear combinations of the different particles' position and momentum, that behave as constants of the motion. For n particles on a string, these constants of the motion are the modes of vibration, and should you want to find the position of any one of the particles, you can expand it in terms of these modes.

To get to field theory, we let the length of the string go to infinity, and the space between particles to zero. Thus, the position of each "particle", a construct we will soon leave behind, is described by a continuous field, $\phi(x)$, and our system has infinitely many degrees of freedom. When we go fom n particles to the continuous case of a field, the Lagrangian is expressed as the integral over space of a Lagrangian density, so

$$S = \int_0^t \mathrm{d}t L = \int_0^t \mathrm{d}t \int_{-\infty}^{\infty} \mathrm{d}^3 \boldsymbol{x} \mathcal{L}$$

The analogue to our classical case still holds up fairly well. The value of a field $\phi(x)$ at a point x is the deviation of a wave function from some equilibrium. The constants of motion described by generalized coordinates are harmonic oscillators vibrating at any one of a continuum of energies. The well known solutions of the quantum mechanical harmonic oscillator involving ladder operators fill the role of describing these modes of vibration on an "infinitely long string", and the ladder operators raising and lowering the energy of the oscillator by an amount ω are interpreted to create or annihilate, respectively, a particle of the appropriate energy. Similarly to the discrete case, the field at a point x can then be expanded in terms of these modes of vibration, by way of a Fourier integral over all momenta k.

As an example, for a massive spin-0 particle we have the Lagrangian density:

$$\mathcal{L} = \partial_\mu \hat{\phi} \partial^\mu \hat{\phi} - \frac{1}{2} m^2 \hat{\phi}^2 \tag{2.1}$$

which when we apply the Euler-Lagrange equations

$$\frac{\partial \mathcal{L}}{\partial \hat{\phi}} - \partial_\mu \left(\frac{\partial \mathcal{L}}{\partial(\partial_\mu \hat{\phi})} \right) = 0$$

result in the proper Klein-Gordon equation of motion.

$$(\Box + m^2)\hat{\phi} = 0$$

Where $\Box$ is the d'Alembertian operator

$$\Box = \partial_\mu \partial^\mu = \frac{\partial^2}{\partial t^2} - \nabla^2$$

and the 'hat' over $\hat{\phi}$ signifies that we have taken the step to a quantized theory by substituting in operators $\hat{a}$ and $\hat{a}^\dagger$ in the expansion

$$\hat{\phi}(x) = \int_{-\infty}^{\infty} \frac{\mathrm{d}^3 \boldsymbol{k}}{\sqrt{2\omega}(2\pi)^3} \left[\hat{a}_k e^{-ikx} + \hat{a}_k^\dagger e^{ikx} \right]$$

The conjugate momentum is

$$\hat{\pi}(x) = \frac{\partial \mathcal{L}}{\partial \dot{\hat{\phi}}} = \int_{-\infty}^{\infty} \frac{\mathrm{d}^3 \boldsymbol{k}}{\sqrt{2\omega}(2\pi)^3} (-i\omega) \left[\hat{a}_k e^{-ikx} - \hat{a}_k^\dagger e^{ikx} \right]$$

From here on out, I will omit the hat from the field and conjugate momenta for the sake of a cleaner notation. Hopefully, it will be clear from the context of a particular π, whether it should be read as a mathematical constant or the conjugate momentum operator. Just like we get a Lagrangian density in the continuum case, we also get a Hamiltonian density,

$$\mathcal{H} = \pi\dot{\phi} - \mathcal{L} = \frac{1}{2}\pi^2 + \frac{1}{2}\left(\frac{\partial\phi}{\partial x}\right)^2$$

so the total Hamiltonian is;

$$H = \int_{-\infty}^{\infty} \mathrm{d}^3\boldsymbol{x}\mathcal{H}$$

The commutation relation

$$[x, p] = i$$

necessarily has a counterpart in field theory. The field ϕ and its conjugate momentum π must satisfy the relation

$$[\phi(x,t), \pi(y,t)] = i\delta(x-y)$$

which translates into the following for the creation and annihilation operators:

$$[a_k, a^\dagger_{k'}] = 2\pi\delta(k-k')$$

Inserting the expansions for ϕ and π in the expression for H, it turns out to have a form analogous to the case of the single harmonic oscillator.

$$H = \frac{1}{2}\int_{-\infty}^{\infty} \frac{\mathrm{d}^3\boldsymbol{k}}{(2\pi)^3}\left[a^\dagger_k a_k + a_k a^\dagger_k\right]\omega$$

2.3 The Interaction Picture and the S-matrix

The fields that obey the equations of motion we get from (2.1) are free. They do not interact, as can be seen from, among other things, the fact that the expansions of the ϕ and π operators take the form of plane-wave solutions. If we want to consider interactions, we shall have to modify our Hamiltonians accordingly. This presents a potential problem, as the uniquely simple nature of the operator expansions are intimately tied to the form of the hamiltonian. After all, the development over time of an operator in the Heisenberg picture $O_H(t)$ is determined by:

$$i\frac{\partial}{\partial t}O_H = [O_H, H_H]$$

This will no longer result in the nice expansion of ϕ and π in plane wave form.

An enticing alternative exists in splitting the Hamiltonian into two parts. H_0 containing the terms pertaining to the free fields, and H_I containing the terms connected to the interaction. We also move to a picture where a state $|S_I\rangle$ is related to the Schrödinger picture state $|S_S\rangle$in the following manner:

$$|S_I\rangle = e^{iH_0 t}\,|S_S\rangle \tag{2.2}$$

The time evolution of a state in the Schrödinger picture is governed by:

$$i\frac{\partial}{\partial t}\,|S_S\rangle = H\,|S_S\rangle$$

and if we insert this into equation (2.2)

$$i\frac{\partial}{\partial t}\,|S_I\rangle = H_I\,|S_I\rangle \tag{2.3}$$

we see that the time evolution of a state in the interaction picture is governed by the interaction part of the Hamiltonian. In order for our predicted observables to be consistent throughout the different pictures we must have

$$\begin{aligned}
\langle S_I|\,O_I\,|S_I\rangle &= \langle S_S|\,O_S\,|S_S\rangle \\
\langle S_S|\,e^{-iH_0 t}O_I e^{iH_0 t}\,|S_S\rangle &= \langle S_S|\,O_S\,|S_S\rangle \\
&\Downarrow \\
O_I &= e^{iH_0 t}O_S e^{-iH_0 t} \\
&\Downarrow \\
i\frac{\partial}{\partial t}O_I &= H_0 O_I
\end{aligned}$$

How fortuitous! In the interaction picture the time evolution of the operator, O_I, is governed solely by the free part of the Hamiltonian, H_0, meaning we get to keep its well-behaved expansion.

We will at some point want to use all of this to predict outcomes of physical processes. So sooner or later we will have to deal with the equations telling us about these processes behaving in a notoriously difficult manner, forcing us off the comfortable path of solutions that are linear combinations of each other. In a time honored tradition we would prefer to:

1. Have some demarcation of when we cross the border where things start to go south, and deal only with a simple approximation until we get to this place.

2. When we absolutely *have* to increase the complexity of things, we want to delve no deeper into nonlinear regions than there is a reason to. Once our answers are deemed close enough, we call it a day.

3. We would like to approach the unknown by way of the known. The well behaved solutions will be nudged and coaxed towards "ugly" territory. As long as we do not press too far, and keep a clear perspective of how wrong we expect to be as a result of our imperfections, we'll probably be OK.

In keeping with this approach, we start out at the time $t = -\infty$, where particles are far apart, and we can expect them to not interact.

$$|i\rangle$$

The particles in this state close on each other and interact, before parting again. Our next snapshot is at $t = \infty$ where particles can again be assumed to be free. Although they will possibly be an entirely different set of particles. We now define S as the operator that takes us from $-\infty$ to ∞.

$$|\infty\rangle = S\,|i\rangle \tag{2.4}$$

The amplitude for starting with a set of paticles in the state $|i\rangle$ and ending with them in a particular final state $|f\rangle$, is then the matrix element S_{fi}.

$$\langle f|\,\infty\rangle = \langle f|\,S\,|i\rangle = S_{fi}$$

We want to figure out how to calculate the S-matrix. We start with integrating eq. (2.3):

$$|t\rangle = |i\rangle - i\int_{-\infty}^{t} \mathrm{d}t_1 H_I(t_1)\,|t_1\rangle$$

Assuming the interaction to be weak, we can approach this in iterations, in a similar manner to normal quantum mechanics. A first iteration is:

$$|t\rangle = |i\rangle$$

Inserting this back into the equation for $|t\rangle$, gives a result correct to the first order in H_I:

$$|t\rangle = |i\rangle - i\int_{-\infty}^{t} \mathrm{d}t_1 H_I(t_1)\,|i\rangle$$

We then repeat this to get something correct in the second order:

$$\begin{aligned}
|t\rangle &= |i\rangle - i\int_{-\infty}^{t} \mathrm{d}t_1 H_I(t_1)\,|t_1\rangle \\
|t\rangle &= |i\rangle - i\int_{-\infty}^{t} \mathrm{d}t_1 H_I(t_1)\left[|i\rangle - i\int_{-\infty}^{t_1} \mathrm{d}t_2 H_I(t_2)\,|i\rangle\right] \\
|t\rangle &= |i\rangle - i\int_{-\infty}^{t} \mathrm{d}t_1 H_I(t_1)\,|i\rangle - \int_{-\infty}^{t}\int_{-\infty}^{t_1} \mathrm{d}t_1 \mathrm{d}t_2 H_I(t_1) H_I(t_2)\,|i\rangle \\
|t\rangle &= \left(1 - i\int_{-\infty}^{t} \mathrm{d}t_1 H_I(t_1) - \int_{-\infty}^{t}\int_{-\infty}^{t_1} \mathrm{d}t_1 \mathrm{d}t_2 H_I(t_1) H_I(t_2)\right)|i\rangle
\end{aligned}$$

Letting t and the number of iterations go to infinity, and comparing with eq. (2.4), we see that we have an expression for the S-matrix.

$$S = \sum_{i=0}^{\infty} (-i)^n \int_{-\infty}^{\infty}\int_{-\infty}^{t_1} \cdots \int_{-\infty}^{t_{n-1}} \mathrm{d}t_1 \cdots \mathrm{d}t_n H_I(t_1) \cdots H_I(t_n)$$

A few more tricks involve recalling that the Hamiltonian is actually an integration over all space of a Hamiltonian density, and exploiting the relationship

$$\int_{-\infty}^{\infty}\int_{-\infty}^{t_1} \cdots \int_{-\infty}^{t_{n-1}} \mathrm{d}t_1 \cdots \mathrm{d}t_n = \frac{1}{n!}\int_{-\infty}^{\infty}\int_{-\infty}^{\infty} \cdots \int_{-\infty}^{\infty} \mathrm{d}t_1 \cdots \mathrm{d}t_n$$

along with the time ordering of our operators, that is, placing earlier operators to the right of later ones. These tricks secure us a new sum for the S-matrix.

$$S = \sum_{i=0}^{\infty} \frac{(-i)^n}{n!} \int_{-\infty}^{\infty} \cdots \int_{-\infty}^{\infty} \mathrm{d}^4x_1 \cdots \mathrm{d}^4x_n T[\mathcal{H}_I(x_1) \cdots \mathcal{H}_I(x_n)] \tag{2.5}$$

There is still quite a way to go before any of this is useful for calculating cross sections. There is no sense in covering it all here, but in any case, we will now consider briefly the nature of the interactions contained in H_I.

2.4 Interaction and Gauge symmetry

Suppose we have a function describing the behaviour of an electron, say, interacting with other electricallly charged particles. That is, under the influence of what would classically be termed the Lorentz force. Will the equations we use to calculate the likelihood of transitions of state be unchanged in nature under a transformation of the vector potential?

$$A^\mu = (V, \mathbf{A}) \rightarrow A'^\mu = A^\mu - \partial^\mu \chi(x)$$

We know that they must be, since when we treat this classically, we have for the physically observable fields [25]:

$$\mathbf{B} = \nabla \times \mathbf{A}$$
$$\mathbf{E} = -\nabla V - \frac{\partial \mathbf{A}}{\partial t}$$

These fields are clearly unimpressed by any transformation of A^μ of the form given, and so our equations of motion for the quantum field description must also be of the same form after such a transformation. We call such a transformation a *Gauge transformation* and say that our Lagrangian must be *Gauge invariant* [26].

Insisting on this gauge invariance means that as A^μ transforms according to its specified pattern, our state function ϕ also has to obey a specific transformation rule:

$$\phi \to \phi' = e^{-iq\chi}\phi$$

We must in addition make the following replacement for any and all operators ∂^μ that show up in the Lagrangian:

$$\partial^\mu \to D^\mu = \partial^\mu + iqA^\mu$$

So we see that if we want gauge invariance, we invalidate the notion of a free field. Any term $\partial_\mu \phi^\dagger \partial^\mu \phi$ that would previously only correspond to the free particles' kinetic energy, will now change into$D_\mu \phi^\dagger D^\mu \phi$, and thus include an interaction term involving a product between A^μ and ϕ.

2.5 Troubles of the Standard Model, and introduction of SUSY

Naturally, and as I have said before, to actually get this approach anywhere worthwhile is considerably more involved than this rudimentary sketch. But even after digging much deeper in order to get a QFT description of the electroweak interaction, there is one thing in particular that stands out as something of a deficit in the result you get from the procedure I've outlined thus far: All the particle in the Lagrangian you end up with are massless, and adding a mass term breaks gauge invariance [2].

To alleviate this inconvenience, one customarily introduces the Higgs field. The Higgs field has a *degenerate* ground state. It still transforms according to the rules of gauge invariance, but as having no quanta of this field present means picking out one of the infinitely many ground states as *the* ground state, symmetry is *spontaneously broken.* Writing out the resulting lagrangian shows that by including this field and its interaction terms, we also pick up mass terms for the other particles[26].

This ingenious solution brings its own set of problems. The idea of eq. (2.5) is that as you include more terms from the sum, your predictions for physical processes should get better. However, in order to avoid divergent integrals from the higher order terms in the sum of two otherwise unrelated parameters of the theory will have to cancel each other out to an extraordinary degree of precision.

Supersymmetry is the notion of introducing a symmetry of the lagrangian between fermions and bosons similar to the one that already exists between particles and antiparticles[27]. As a matter of design, this symmetry has the cancellation of the mentioned parameters embedded in it as a feature. In the introduction, I mentioned that since we have not found any boson that is otherwise extraordinarily similar to an electron, we must assume supersymmetry to be broken.

You can keep going into exactly how this may happen without removing the desireable feature of solving the divergence problem, and how we end up with a theory that has a rather unwieldy number of experimentally determined parameters, not all combinations of which are physically interesting. But we will not. I shall simply establish that picking out a reasonable set of parameters and determining the particle's resultant expectant behavior is a huge task. For my purposes, I will simply make use of the work of Ibarra/Tran [28], who operate with a gravitino and a degree of R-parity breaking that results in a mean life of $\tau_{\tilde{g}} = 2e26$ s, a mass of 150 GeV, and with a branching ratio of 0.05 decays to a gamma ray and a neutrino.

Chapter 3

Galactic contribution to the gamma flux

3.1 The shape of the galactic flux

The *gravitino* is the hypothetical sister particle of the *graviton*, the mediator of gravitational force (itself at the moment not confirmed). Its exact characteristics depend on the parameters of the SUSY-model you're examining, but as the sparticle connected to the graviton, its spin is set at 3/2.

If you set your parameters so that the gravitino is the LSP, and the R-parity only slightly broken, you can end up with a gravitino that decays to Standard Model particles with a mean life in the neighborhood of the age of the universe. That could then mean that it is still present in large enough amounts to fill the role as Dark Matter, while at the same time still turning into something we can actually measure once in a great while.

What we're looking for now is a way to express the energy received here on earth from gravitino decays, in a manner that lets us compare to the data we have. Let's see what happens if we assume for the moment that the gravitino decays to a single product involving a gamma ray and some other particle. Specifically, we will be talking about the decay:

$$\tilde{g} \to \gamma\nu$$

Since the neutrino has negligible mass, considerations of energy and momentum tell us that exactly half the energy will be released as a photon ($E_0 = m_{\tilde{g}}/2$). There are other possibilities of course, but we're keeping things simple.

It behooves me now to mention what I am going to use at the end of all this in order to compare my ramblings to reality: EGRET, or the Energetic Gamma-Ray Experiment

Telescope, was, as the name implies, a telescope designed for detecting γ-rays placed on the Compton Gamma Ray Observatory, a satellite observatory designed for the examination of the high energy universe. Its readings of average flux in the relevant energy range are displayed in figure 3.1, as presented by [29]. EGRET's energy resolution in this range is 15% [28].

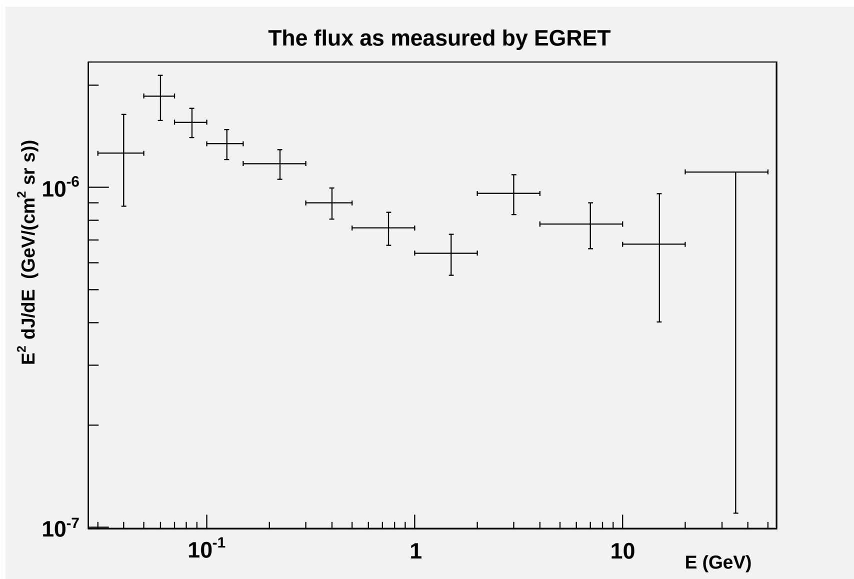

Figure 3.1: EGRET-data - The average flux for our relevant energy range, as collected by EGRET [29].

Say the gravitino has an average life time $\tau_{\tilde{g}}$. Then the number of gravitinos decaying per unit time in a volume containing N gravitinos is $N/\tau_{\tilde{g}}$. The relevant amount of energy ΔE in a small volume ΔV is determined by multiplying ΔV by the Dark Matter Energy Density. Let's just call it ρ:

$$\Delta E = \rho \Delta V$$

The number of gravitinos in ΔV is found by dividing the energy contained by the mass of the gravitino $m_{\tilde{g}}$:

$$\Delta N = \frac{\rho \Delta V}{m_{\tilde{g}}}$$

These gravitinos disappear at a rate proportional to the inverse of their mean life $\tau_{\tilde{g}}$,

$$\frac{\mathrm{d}\Delta N}{\mathrm{d}t} = \frac{-\rho \Delta V}{m_{\tilde{g}} \tau_{\tilde{g}}} \tag{3.1}$$

Let me state ΔV explicitly, as we let it go to the infinitesimal volume element dV: Let a point be located at (s, b, l), s, b, and l being distance from earth and galactic latitude and longitude, respectively (figure 3.2). Then we have for the volume element at this point:

$$dV = s^2 \cos b \, ds \, db \, dl$$

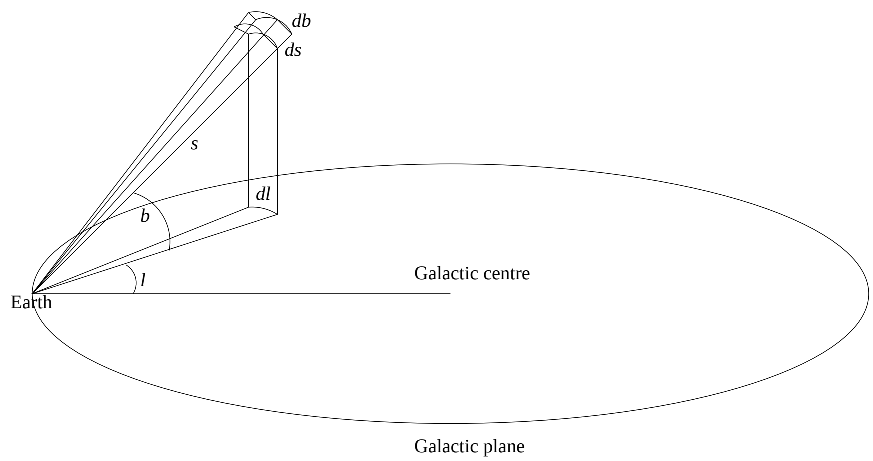

Figure 3.2: The galactic coordinate system - A representation of what it means that a point has the galactic coordinates (s, b, l), as well as as visualization of the infinitesimal volume $dV = s^2 \cos b \, ds \, db \, dl$.

To find the energy sent towards us, we remove the minus sign from (3.1) and multiply with the appropriate energy per decay. The energy released as a photon by each decaying gravitino is E_0, but EGRET will register this as a Gaussian distribution with a spread determined by its resolution. In addition, the energy released will be spread over an area $1/4\pi s^2$. Accordingly, we multiply eq. (3.1) by

$$\frac{1}{4\pi s^2} \frac{1}{\sqrt{2\pi}\sigma} \exp\left[\frac{-(E - E_0)^2}{2\sigma^2}\right]$$

where the Gaussian width σ is proportional to the central value E_0:

$$\sigma = \frac{0.15 E_0}{2\sqrt{2\ln 2}}$$

Define J to be the number of photons that reaches us per unit area, per solid angle, and per unit time. It will be a function of the energy of the photons in question of course.

The flux from dV then, in so many words: The total amount of energy released from the volume dV, at a position s, l, b, that reaches a unit area at EGRET per unit time, *as read* by the EGRET instrument (whew!), is:

$$\left(\frac{\mathrm{d}J}{\mathrm{d}E}\right)_{dV}(E) = \frac{1}{4\pi m_{\tilde{g}}\tau_{\tilde{g}}}\frac{1}{\sqrt{2\pi}\sigma}\exp\left[\frac{-(E-E_0)^2}{2\sigma^2}\right]\rho(s,b,l)\cos b\, ds\, dl\, db \tag{3.2}$$

It is also customary to multiply the flux by a power of E to emphasize its spectral nature [30].

By now we have indentified a great deal of what determines any flux of gamma radiation resulting from gravitino decay as we see it on earth. But there is one big part left. I have said nothing of the characteristics of the dark matter distribution in our galaxy, and its effect on measurements. How do we determine ρ? That's next.

3.2 Dark Matter distribution in the Milky Way

No matter how you go about looking for dark matter in the cosmos, it will be essential to have some idea concerning exactly how much you expect there to be of it in any given spot you happen to look.

Any signals from far enough away, we might be able to model as being the result of Dark Matter that is evenly distributed throughout the universe. After all, the universe is homogenous and isotropic on large scales. What this means is that the universe looks the same in all directions and from any viewpoint [31]. But how can this be, you ask? Surely, the Milky Way contains stars aplenty, as does that galaxy just over yonder. All the while, the space between has, in comparison, roughly the dust content of a good sneeze. Homogenous you say? But you will notice that I said on *large* scales. In this context, that means that our yardstick is roughly the size of galaxy *clusters*. So that's all right then.

While taking advantage of the homogeneity of the universe is fine for signals originating outside the Milky Way, the signals from our own galaxy is another matter entirely. Not being situated in the very centre of the Milky Way is all very nice if your concerns are of a more pedestrian variety. Like surviving. But when you want a nice and clean expression for exactly how much radiation reaches you as a result of gravitino decay, it is decidedly impractical. Since the density of Dark Matter is anything but uniform on such comparatively small scales, you need to describe its distribution somehow.

Finding solid footing for such information about hypotheticals is not a trivial task. Simulations like the Millenium Run are a good place to start. The Millenium simulation was meant to check if our current cosmological models can accurately reproduce a universe similar to the one we live in [32]. Starting with initial conditions meant to replicate what we think the universe looked like immediately after the Big Bang, and letting it all unfold according to our current perception of the rules, the simulation ends up with a distribution of particles that can be compared to observation. Considering the success of this simulation and other, older, but similar ones, we may be justified in the hope that a formula that describes the Dark Matter halo of a simulated Milky Way, describes the Dark Matter of the *actual* Milky Way as well.

There have been a few formulas suggested as the best way of modelling the distribution of Dark Matter in simulated galaxies (and therefore hopefully in the real ones): The Navarro-Frenk-White(NFW) and Einasto density profile are both regarded as reasonably successful. NFW suggested the profile

$$\rho_{\text{halo}}(r) \simeq \frac{\rho_h}{\frac{r}{r_c}\left(1+\frac{r}{r_c}\right)^2} \tag{3.3}$$

in 1996 [33]. The parameters ρ_h and r_c must be determined on a case by case basis to fit the galaxy in question. To describe the Milky Way, we will use $\rho_h = 0.33$ GeV cm^{-3} and $r_c \simeq 20$ kpc [28]. The NFW profile is very good at describing the Dark Matter halos resultant from simulations like the Millennium run, and is regularly used for this purpose. Some slight but systematic discrepancies have cropped up as the simulations have gotten bigger though, and the Einasto profile has been fronted as an alternative meant to be as good as, or better than, NFW [34, 35]. It looks like this:

$$\left(\ln\frac{\rho_{\text{halo}}}{\rho_{-2}}\right) = -\frac{2}{\alpha}\left[\left(\frac{r}{r_{-2}}\right)^{\alpha} - 1\right]$$

or

$$\rho_{\text{halo}}(r) = \rho_{-2}\text{exp}\left\{\frac{-2}{\alpha}\left[\left(\frac{r}{r_{-2}}\right)^{\alpha} - 1\right]\right\} \tag{3.4}$$

The parameters of the Einasto profile are related to NFW by $r_{-2} = r_c$ and $\rho_{-2} = \rho_h/4$ [35]. For galaxy-sized halos, a reasonable value for α is $\alpha \approx 0.172 \pm 0.032$ [34]. The Einasto profile has a few other desirable qualities as well. It does not diverge as $r \to 0$, and also, as its density cuts of exponentially at large r, it has a finite total mass [36].I will be using the Einasto profile from here on out. Let's use a figure to visualize what such a distribution of Dark Matter in our galaxy means (figure 3.3):

Since these profiles depend on r only, an observer situated in the centre of the Milky Way would perceive any signal from the decay of Dark Matter as completely isotropic (If our model is rooted in reality, that is). Earthlings, perched precariously at the tip of a spiral arm, are not so lucky. Any signal we get will be from the decay of a gravitino located a

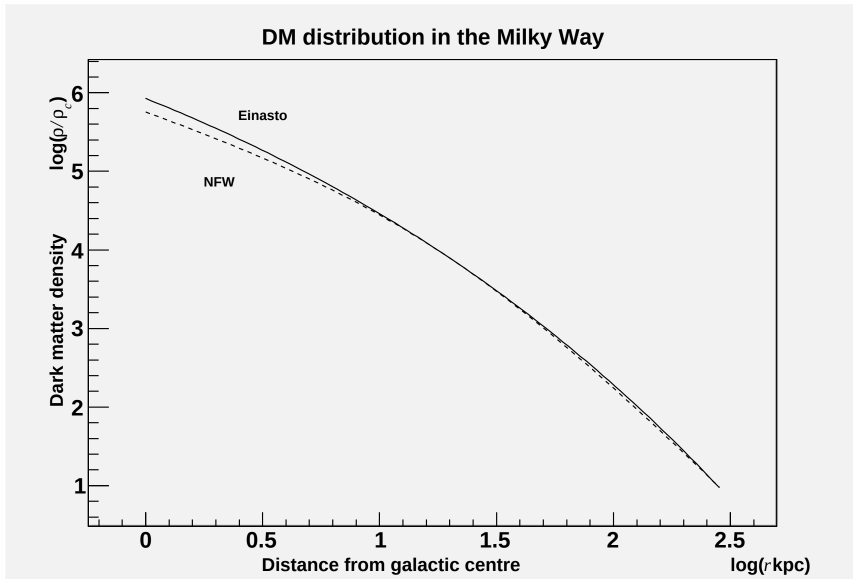

Figure 3.3: Density profile - The Dark Matter density as a function of the distance r from the galactic centre of the milky way. The line plot is the Einasto profile, while the dashed plot is NFW.

distance s from the earth. Calculating the sum total of the expected signal from any one direction will necessitate integrating over all contributions. From Dark Matter situated at $s = 0$ all the way until we get so far away that any further contributions from the Milky Way is deemed insignificant due to the density being too low. Expressing r as a function of s, we get from figure 3.4:

$$r = \sqrt{R^2 + s^2 - 2Rs\cos l \cos b}$$

where R is the distance from the earth to the centre of the Milky Way. Let's say that we have a distance r_t where we deem the Dark Matter density too low to be of any significance. Call it the truncation radius. Taking the positive root of the quadratic equation for s yields:

$$s_t = R\cos l \cos b + \sqrt{(R\cos l \cos b)^2 + (r_t^2 - R^2)}$$

As the density of a dark matter halo decreases exponentially for $r \to \infty$, it is not as crucial to pick an "accurate" truncation radius as it might have been for the NFW distribution with its divergent total mass. The main point is to go far enough that the impact of r_t is negligible as compared to the inaccuracies of the EGRET-data. $r_t = 15r_{-2}$ will be quite sufficient. So in order to find the total signal originating from our own galaxy in a direction l, b, we need to integrate:

$$\int_0^{s_t} \rho[r(s, l, b)]\mathrm{ds}$$

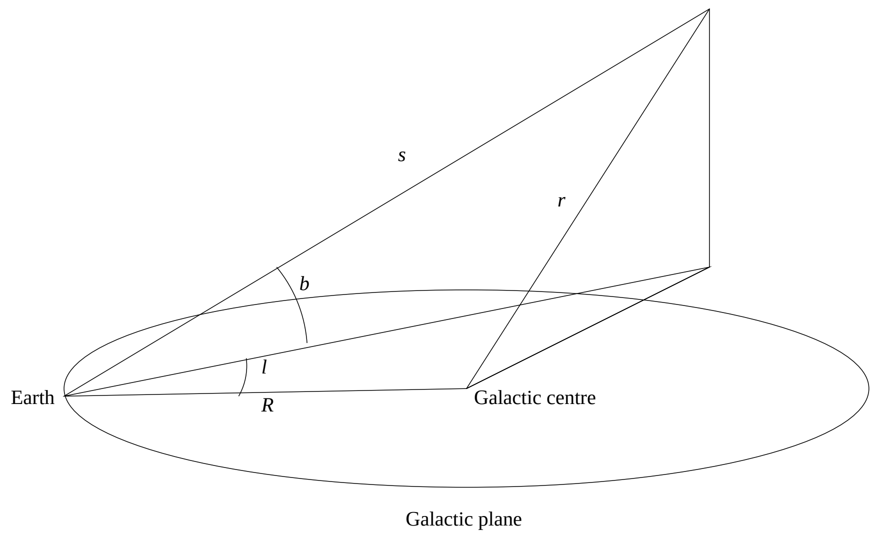

Figure 3.4: A matter of perspective - This figure shows the relation between a point located at (s, b, l) and its distance from the galactic centre , r.

Expanding this integral to describe a volume contained by $0 \leq s \leq s_t$ and the solid angle Ω_Δ, and including the necessary constants from equation (3.2), we finally have an expression for the average flux [28].

$$E^2 \frac{\mathrm{d}J}{\mathrm{d}E} = \frac{E^2}{4\pi\sqrt{2\pi}\sigma m_{\tilde{g}} \tau_{\tilde{g}} \Omega_\Delta} \exp\left[\frac{-(E-E_0)^2}{2\sigma^2}\right] \int_0^{s_t} \int_{\Omega_\Delta} \rho[r(s,b,l)] ds d\Omega \; \frac{\mathrm{GeV}}{\mathrm{cm^2 sr\ s}} \tag{3.5}$$

where

$$d\Omega = \cos b \, db \, dl$$

Evaluating the integral numerically, we get the average flux as a function of E. This is plotted in figure 3.5 for the values mentioned in the previous chapter: $m = 150$ GeV, $\tau_{\tilde{g}} = 2 \cdot 10^{26}$ s, and with a Branching Ratio of 0.05.

There've been some concessions made that could bear further scrutiny. First of all, I mentioned that while it's impossible to numerically evaluate our integral all the way to infinity, the fact that it converges for large r allows us to simply evaluate it to a suitably large truncation radius r_t. We deem any contribution made beyond this radius to be negligible. From figure 3.6 we see that a truncation radius of 14 times the scale radius fulfills this requirement admirably.

The center of our domain also gives us trouble. While the Einasto model is well-behaved for $r = 0$, to actually examine numerically such a wide range of numbers is very cumbersome. And the NFW model actually can not be evaluated at the center. So again, there are parts

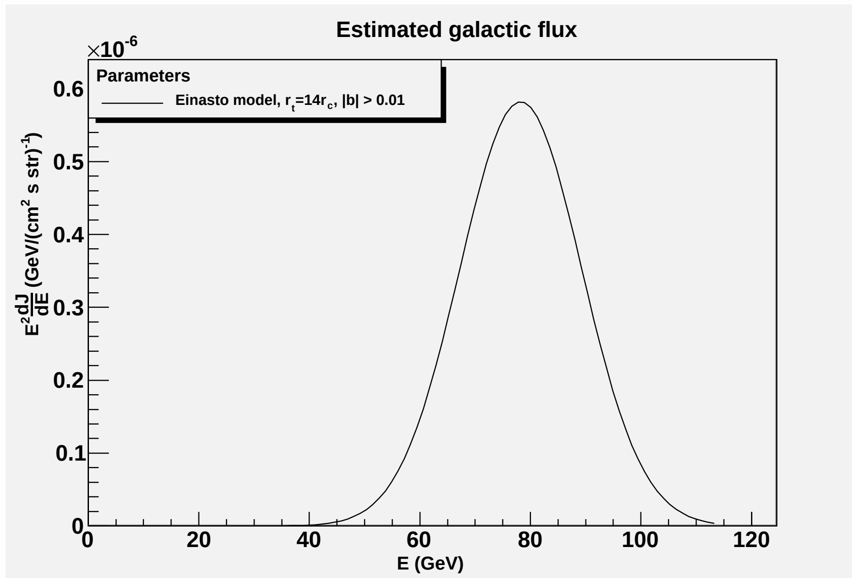

Figure 3.5: Galactic flux - The expected values of the γ-ray flux of galactic origin from a gravitino with $m = 150$ GeV, $\tau_{\tilde{g}} = 2e26$ s, and decaying to a photon and a neutrino with a Branching Ratio 0.05. Although none of these things will change within *this* chapter, other things, such as the distribution mode, will. This is the "default" model configuration, compared with others in the following figures in this chapter.

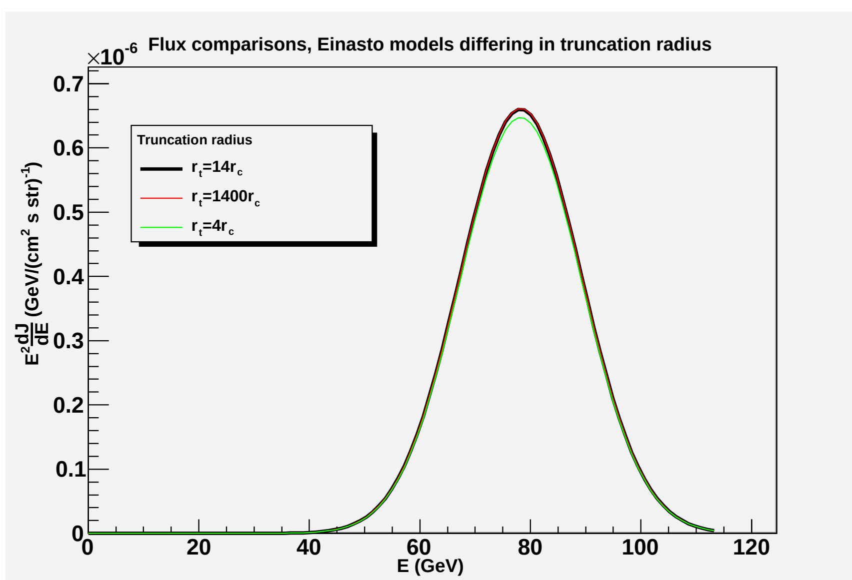

Figure 3.6: Truncation radius comparison - The different computed fluxes for the Einasto model evaluated at different truncation distances.

we want to skip, or at least simplify, and so we need to know what, if any, difference there is between our adaptations and what we would get if we didn't modify our models in such a manner. Figure 3.7 shows that even if instead of skipping the parts closest to the galactic

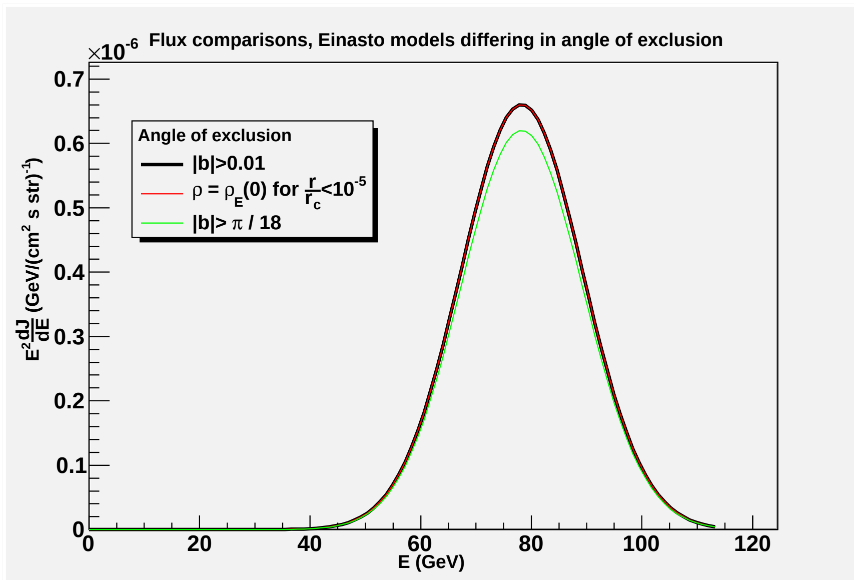

Figure 3.7: Angle of exclusion comparison - The different computed fluxes for the Einasto models excluding different neighborhoods of the galactic disk.

disk (including only the parts where the galactic latitude $|b| > 0.01$), we overestimate them by setting them equal to $\rho(0)$, we get no significant extra contribution. As simply skipping these parts is much less labor intensive, it is what I have ended up doing.

Finally, it could be nice to examine the predicted flux for different models using otherwise similar parameters. Looking at this comparison in figure 3.8 we se that there actually is a difference, but not anything big enough to have much of a say compared to the accepted uncertainties from EGRET's measurements. As far as other models are concerned, we will discuss them in the next section.

From the figures, we see that the expected flux do not contradict the data from EGRET, as well we would hope, seeing as this so far has been mostly a reproduction of litterature that argues for the plausibility of this scenario. But the understanding of what influences the galactic flux will come in handy later.

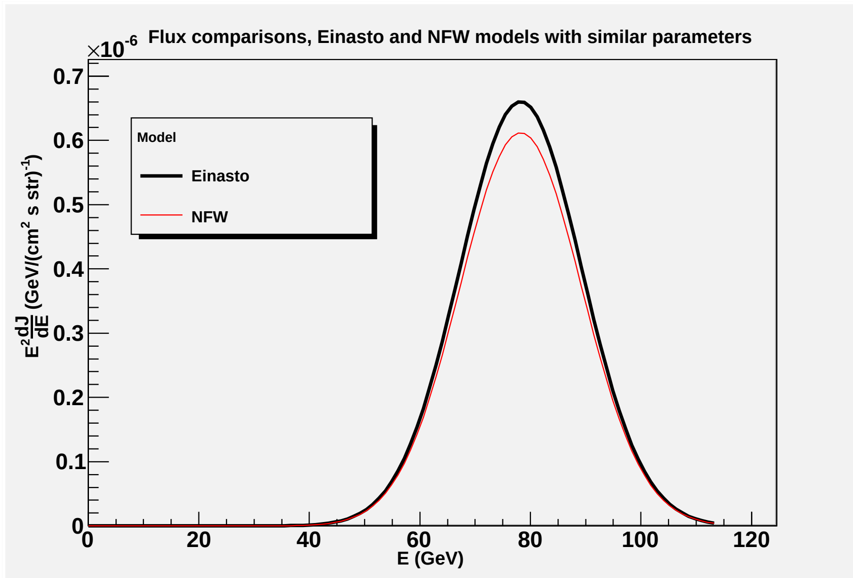

Figure 3.8: Model comparison - The different computed fluxes for two different models using the same angle of exclusion, along with truncation and scaling radius.

3.3 The impact of models

A variety of models have been proposed and examined when it comes to describing matter distribution in halos. D. Merritt et al discuss the relative merits of several of them in their paper *E*mpirical Models for Dark Matter Halos. I. Nonparametric Construction of Density Profiles And Comparison With Parametric Models. Different models are suited for different tasks. Some excel at describing galaxy-sized halos, while others are better at cluster-sized. But all the models examined in this paper share one thing: They are designed to fit simulated models, and can not be carelessly applied to a real world example. And yet we will try to say something about the sensitivity to our choice of model, based on these simulated densities.

As of yet, there is no theoretically motivated model that has been shown to generally describe a dark matter halo at an arbitrary scale. So instead we have this collection of models with free parameters that can be tweaked to fit individual cases.

As a couple of examples we have the (α, β, γ) model from L. Hernquist [37]:

$$\rho(r) = \rho_s 2^{(\beta-\gamma)/\alpha} \left(\frac{r}{r_s}\right)^{-\gamma} \left[1 + \left(\frac{r}{r_s}\right)^{\alpha}\right]^{(\gamma-\beta)/\alpha}$$

This model is equivalent to the NFW model for $(\alpha, \beta, \gamma) = (1, 3, 1)$. And there is the

Prugniel-Simien [38] model:

$$\rho(r) = \rho_p \left(\frac{r}{R_e}\right)^{-p} \exp\left[-b\left(\frac{r}{R_e}\right)^{1/n}\right]$$

ρ_p, ρ_s, α, b and so on are examples of the parameters that are used to fit the model to a distribution.

Merritt et al. determined goodness of fit by:

$$\Delta^2 \equiv \frac{\sum_{j=1}^{m} \delta_j^2}{m-3}$$

$$\delta_j = \log\left[\frac{\hat{\rho}(r_j)}{\rho_{param}(r_j)}\right]$$

where $\hat{\rho}(r_j)$ is the distribution density at points r_j distributed uniformly in $\log(r)$. $\rho_{param}(r_j)$ is the parametrized density model evaluated at the same points.

Typical values of Δ for galaxy-sized halos are $\Delta \sim 0.03$. Since Δ is a rms value, higher than average values of δ_j will increase Δ disproportionately, meaning that if we assume that all δ_j are equal, we will tend to overestimate them. Setting $\delta_j < 0.035$, we get:

$$0.923 \cdot \rho_{param} < \hat{\rho} < 1.083 \cdot \rho_{param}$$

This suggests that the differences to be expected between two reasonably well fitted models should not be all that great, although in Merritt's paper the Einasto profile did perform best overall, and especially well on galaxy-sized halos. And even if models may not turn out to be spot on in the real world, we will see later that in the context that we're interested in, which will be trying to manipulate the relation between galactic and extragalactic flux, differences that are this order of magnitude turn out to be not so important after all.

Chapter 4

Extragalactic contributions to the gamma flux

To figure out what flux to expect from sources *not* in the galaxy, poses a set of challenges different from the local case. The differences are due to a consideration of scale. As already mentioned, the universe is homogenous and isotropic on large scales, and for the duration of this chapter, the scale shall be well and truly large. This being the case, we need no longer concern ourselves with a difference due to direction. Every direction is the same. However, the universe is expanding, and as it expands, light is *redshifted* to lower energies. Meaning that a photon starting its journey packing an energy E, will be noticably less energetic by the time it reaches us. While figuring out how this affects us, we will be dealing with a lot of concepts from the framework of general relativity, and an overview of these concepts can be found in "Gravity: An Introduction to Einstein's General Relativity" by James B. Hartle [31].

4.1 Einstein's equations in the RW-metric

A good place to start is Einstein's equations, relating the curvature of space to its mass energy density:

$$R_{\mu\nu} - \frac{1}{2}g_{\mu\nu}R - \Lambda g_{\mu\nu} = 8\pi G T_{\mu\nu} \tag{4.1}$$

We will now spend some time examining the parts of this equation, starting with defining a metric. We will use the Robertson Walker metric describing the geometry of a homogenous and isotropic universe.

$$g_{\mu\nu} = \begin{pmatrix} 1 & 0 & 0 & 0 \\ 0 & \frac{-a^2}{1-kr^2} & 0 & 0 \\ 0 & 0 & -a^2r^2 & 0 \\ 0 & 0 & 0 & -a^2r^2\sin^2\theta \end{pmatrix}$$

or equivalently

$$ds^2 = dt^2 - a^2(t)\left[\frac{dr^2}{1-kr^2} + r^2(d\theta^2 + \sin^2\theta d\phi^2)\right]$$

where ds is the line element in terms of the comoving coordinates r, θ, and ϕ, and a is the scaling factor, a measure of the expansion of the universe. Something that is moving along with an expanding universe has constant comoving coordinates. The increase in proper distance is contained in a. Since a is normalized to be one at the present time, present comoving distance is equal to present proper distance.

The parameter k depends on the curvature of the universe. It is $+1$, 0, or -1 for a closed, flat, or open universe, respectively.

It is also useful to know the inverse of the metric, $g^{\mu\nu}$. Luckily, since $g_{\mu\nu}$ is diagonal, the simple relation $g^{\mu\nu} = 1/g_{\mu\nu}$ is valid for each component.

Λ is the *cosmological constant*, playing the role of the intrinsic energy density, and associated negative pressure, of the vacuum of empty space [39]. G is Newton's gravitational constant.

$T_{\mu\nu}$ is the *stress-energy tensor*. Its components denote the flux of the μ component of the momentum 4-vector across the surface with a constant x^ν coordinate. Letting a latin index denote a spatial component, this means that $T_{\mu 0}$ is associated with energy-momentum density, T_{0i} with energy flux, T_{ii} with pressure, and the remaining non-diagonal spatial terms, $T_{ij}, i \neq j$, represent shear stress. Our homogenous and isotropic universe can be modelled in a satisfactory fashion as a perfect fluid. In this case all non-diagonal terms vanish, and we're left with

$$T_{\mu\nu} = \begin{pmatrix} \rho & 0 & 0 & 0 \\ 0 & p & 0 & 0 \\ 0 & 0 & p & 0 \\ 0 & 0 & 0 & p \end{pmatrix}$$

A set of generally useful quantities called *Christoffel symbols* are defined in terms of the metric, thus:

$$\Gamma^{\alpha}_{\mu\nu} = \frac{g^{\rho\alpha}}{2}\left(g_{\nu\rho,\mu} + g_{\mu\rho,\nu} - g_{\nu\mu,\rho}\right)$$

where $g_{\mu\nu,\rho}$ means that $g_{\mu\nu}$ should be partially differentiated with respect to x^ρ. Note that using Einstein's summation convention, indices that are written as a sub and superscript, both in the same term, are taken to be summed over. I will calculate an example, Γ^0_{11} explicitly, and list the rest of the non-zero Christoffel symbols for the RW-metric in appendix B.

$$\Gamma^0_{11} = \frac{g^{00}}{2}(\partial_1 g_{10} + \partial_1 g_{10} - \partial_0 g_{11}) = \frac{-g^{00}\partial_0 g_{11}}{2} = \frac{a\dot{a}}{1-kr^2}$$

Using Christoffel symbols, we can now, in turn, define the *Riemann curvature tensor*. As before there follows the explicit calculation of one component, and the rest are found in appendix B:

$$R^\alpha_{\beta\gamma\delta} = \Gamma^\alpha_{\beta\delta,\gamma} - \Gamma^\alpha_{\beta\gamma,\delta} + \Gamma^\alpha_{\rho\gamma}\Gamma^\rho_{\beta\delta} - \Gamma^\alpha_{\rho\delta}\Gamma^\rho_{\beta\gamma}$$

$$\begin{aligned}
R^0_{101} &= \Gamma^0_{11,0} - \Gamma^0_{10,1} + \Gamma^0_{\rho 0}\Gamma^\rho_{11} - \Gamma^0_{\rho 1}\Gamma^\rho_{10} \\
&= \frac{\dot{a}^2 + a\ddot{a}}{1-kr^2} - 0 + 0 - \frac{a\dot{a}}{1-kr^2}\frac{\dot{a}}{a} \\
&= \frac{a\ddot{a}}{1-kr^2}
\end{aligned}$$

There are other non-zero components than those listed, but keeping in mind that indices can be lowered

$$R_{\alpha\beta\gamma\delta} = g_{\alpha\mu}R^\mu_{\beta\gamma\delta}$$

they can all be found using the following identities:

$$R_{\alpha\beta\gamma\delta} = -R_{\beta\alpha\gamma\delta}$$

$$R_{\alpha\beta\gamma\delta} = -R_{\alpha\beta\delta\gamma}$$

$$R_{\alpha\beta\gamma\delta} = +R_{\gamma\delta\alpha\beta}$$

$$R_{\alpha\beta\gamma\delta} + R_{\alpha\delta\beta\gamma} + R_{\alpha\gamma\delta\beta} = 0$$

For the components we need, it is easy to facilitate a direct comparison with the ones we already got:

$$R^\alpha_{\beta\gamma\delta} = g^{\alpha\mu}R_{\mu\beta\gamma\delta} = -g^{\alpha\mu}R_{\mu\beta\delta\gamma} = -R^\alpha_{\beta\delta\gamma}$$

The first of the quantities actually appearing explicitly in our equation is $R_{\mu\nu}$, the *Ricci curvature tensor*, and with the help of $R^\alpha_{\beta\gamma\delta}$, we write it in the following manner:

$$R_{\mu\nu} = R^\alpha_{\mu\alpha\nu}$$

We arrive at the following components for the Ricci curvature tensor:

$$R_{\mu\nu} = \begin{pmatrix} -\frac{3\ddot{a}}{a} & 0 & 0 & 0 \\ 0 & \frac{a\ddot{a}+2(\dot{a}^2+k)}{1-kr^2} & 0 & 0 \\ 0 & 0 & r^2[a\ddot{a}+2(\dot{a}^2+k)] & 0 \\ 0 & 0 & 0 & r^2\sin^2\theta[a\ddot{a}+2(\dot{a}^2+k)] \end{pmatrix}$$

By now, it will come as no surprise that the last of the mysterious symbols to be computed is derived from $R_{\mu\nu}$. The *Ricci scalar*, as R is called, is calculated like this:

$$R = g^{\mu\nu}R_{\mu\nu} = R^{\mu}_{\mu} = -6\frac{a\ddot{a} + \dot{a}^2 + k}{a^2}$$

Quite a few of the quantities dealt with in this section depend explicitly on time. In cases like this, a variable f_0 is usually taken to mean $f(t = 0)$, and you might be forgiven for thinking that a_0 signifies the value of a at the time of the Big Bang. Not so: In our current context a variable adorned with the subscript (0) represents its value at the present moment.

For additional entertainment value, we will also be handling variables with the subscript (00), which doesn't relate to time at all. Rather, as can be seen above, it can be thought of as the component in the upper left corner of a matrix.

Before we move on, allow me to define Hubble's parameter, H, in terms of a. After all, they're both supposed to say something about the expansion of the universe. We start with the distance seperating two objects, $l(t) = l_0 a(t)$. Then we look at how to express the speed at which two objects a distance l apart recede from each other, $v(t)$,

$$\begin{aligned} v(t) &= \frac{dl}{dt} \\ &= l_0\frac{da}{dt} \\ &= l_0 a(t)\frac{\dot{a}}{a} \\ &= l(t)\frac{\dot{a}}{a} \\ &= H(t)l(t) \end{aligned}$$

where we define

$$H = \frac{\dot{a}}{a} \tag{4.2}$$

That is, the rate at which distant galaxies recede is proportional to their distance from us, with Hubble's parameter as the proportionality factor.

Looking at the 00 component of Einstein's equations (4.1), we write it

$$\left(\frac{\dot{a}}{a}\right)^2 + \frac{k}{a^2} = \frac{8\pi G\rho}{3} + \frac{\Lambda}{3}$$

That is, subtituting in all the values we have so painstakingly calculated. I am going to assume a flat universe, causing the k-term to vanish. This is what is known as the first Friedmann equation [40].

When we next want to solve for one of the spatial dimensions in order to get the 2nd Friedmann equation, it turns out things will be much more straightforward if we change to an orthonormal, as opposed to coordinate, basis.

$$\begin{aligned}
(\mathbf{e}_{\hat{0}})^{\alpha} &= (1,0,0,0) \\
(\mathbf{e}_{\hat{1}})^{\alpha} &= \left(0, \tfrac{\sqrt{1-kr^2}}{a}, 0, 0\right) \\
(\mathbf{e}_{\hat{2}})^{\alpha} &= \left(0, 0, \tfrac{1}{ar}, 0\right) \\
(\mathbf{e}_{\hat{3}})^{\alpha} &= \left(0, 0, 0, \tfrac{1}{ar\sin\theta}\right)
\end{aligned}$$

The components of the Riemann curvature tensor in terms of this new basis are obtained via this transformation:

$$R^{\hat{\alpha}}_{\hat{\beta}\hat{\gamma}\hat{\delta}} = R^{\alpha}_{\beta\gamma\delta}(\mathbf{e}^{\hat{\alpha}})_{\alpha}(\mathbf{e}_{\hat{\beta}})^{\beta}(\mathbf{e}_{\hat{\gamma}})^{\gamma}(\mathbf{e}_{\hat{\delta}})^{\delta}$$

The 2nd Friedmann equation can be found by substituting in one of the spatial parts of Einstein's field equations in this new basis, such as for instance the $\hat{1}\hat{1}$-component.

$$\begin{aligned}
R_{\hat{1}\hat{1}} - \frac{1}{2}\eta_{\hat{1}\hat{1}}R - \eta_{\hat{1}\hat{1}}\Lambda &= T_{\hat{1}\hat{1}} \\
\frac{a\ddot{a} + 2(\dot{a}^2 + k)}{a^2} - \frac{3(a\ddot{a} + \dot{a}^2 + k)}{a^2} + \Lambda &= 8\pi G p \\
-\frac{2\ddot{a}}{a} - \frac{(\dot{a}^2 + k)}{a^2} &= 8\pi G p - \Lambda \\
-\frac{2\ddot{a}}{a} - \frac{(8\pi G\rho + \Lambda)}{3} &= 8\pi G p - \Lambda \\
\frac{\ddot{a}}{a} &= -4\pi G\left(\frac{\rho}{3} + p\right) + \frac{\Lambda}{3} \qquad (4.3)
\end{aligned}$$

where we have used the 1st Friedmann equation to get from line three to four. Since $\eta_{\hat{0}\hat{0}} = g_{00}$ and $R^{\hat{i}}_{\hat{0}\hat{i}\hat{0}} = R^{i}_{0i0}$ for $i = 1, 2, 3$ the first Friedmann equation is unchanged.

4.2 Relations between the Friedmann equations, observables, and other items of interest

We will eventually want to write these equations in a slightly different form, and to this end I'd like to define, and subsequently get to know, a few new parameters. First up, the redshift, z, is expressed in terms of the relation between the current size of the universe, a_0, and its size at the time of emission of the light currently observed, $a(t_e) = a_e$:

$$1 + z = \frac{a_0}{a_e}$$

Since redshift is expressed in this manner, it follows that any redshift will correspond to a certain time of emission, t_e, as well as the distance, at t_0 and t_e, to the object that emitted the light. We will soon take a closer look at some of these relations.

Before we proceed, some new parameters will enable us to ease up on the writing later on. First, we examine the evolution of matter density in the universe. Since the universe is taken to be homogenous, it means that if we have a mix of matter that is largely stable, the amount of such a mix that we can find in a comoving volume must be constant. That is [40]

$$\rho(ar)^3 = constant \Rightarrow \rho = \rho_0(1+z)^3$$

We will assume that the present matter density, ρ_0, equals that of the *critical density*, ρ_c. This determines that we have a flat geometry.

Since we're working with a dark matter candidate that is *almost* stable, it's better if we take this into account. Baryonic matter is still viewed as stable, but dark matter is assumed to decay with a mean life $\tau_{\tilde{g}}$. We use the familiar function for exponential decay,

$$N(t) = Ne^{-t/\tau_{\tilde{g}}}$$

but shifted so that the present day dark matter density, ρ_{DM0}, can be utilized as N, as it is a known parameter:

$$\rho_b = \rho_{b0}(1+z)^3$$

$$\rho_{DM} = \rho_{DM0}(1+z)^3 e^{\frac{-(t-t_0)}{\tau_{\tilde{g}}}}$$

$$\rho = \rho_b + \rho_{DM}$$

$$\rho_0 = \rho_{b0} + \rho_{DM0} = \rho_c$$

At a later stage, as we express t in terms of redshift, that $t(z)$ function will be substituted for t whenever the exponential decay shows up in the expression for a relevant observable.

We now write the first Friedmanns equation

$$\left(\frac{\dot{a}}{a}\right)^2 = \frac{8}{3}\pi G\rho + \frac{\Lambda}{3}$$

in terms of the density parameters

$$\Omega_b = \frac{8\pi G\rho_{b0}}{3H_0^2}$$

$$\Omega_{\tilde{g}} = \frac{8\pi G\rho_{DM0}}{3H_0^2}$$

$$\Omega_\Lambda = \frac{\Lambda}{3H_0^2}$$

For future reference, we also define:

$$\Omega_M = \frac{8\pi G\rho_0}{3H_0^2}$$

So the first Friedmann equation now looks like this:

$$H^2 = \left(\frac{\dot{a}}{a}\right)^2 = H_0^2\left[(1+z)^3\left(\Omega_b + \Omega_{\tilde{g}} e^{\frac{-(t-t_0)}{\tau_{\tilde{g}}}}\right) + \Omega_\Lambda\right]$$

4.2.1 The relation between redshift and measured energy

The relation between redshift and the energy of the photon when received, E_0, versus that at time of emission E_e is fairly simple. A wave that has propagated for so long that space is now twice as big as when it started will have doubled its wavelength, and therefore halved its energy. As the present energy is a function of redshift, we will name it as suc,: $E_0 = E(z)$. We have:

$$\begin{aligned} \frac{\lambda_0}{\lambda_e} &= \frac{a_0}{a_e} \\ \frac{E_e}{E(z)} &= 1+z \\ E(z) &= \frac{E_e}{1+z} \end{aligned} \tag{4.4}$$

Figure 4.1 shows the energy measured, E_0, when a photon originally released with an energy E_e equal to 75 GeV, is received at a redshift z.

4.2.2 The relation between redshift and time

An expression for the time of emission of a photon as a function of redshift can be found by way of the Friedmann equations [41, 42]. We assume a flat, matter dominated (*pressureless*) universe, and add twice the second Friedmann equation to the first:

$$\frac{2a\ddot{a} + \dot{a}^2}{a^2} = \Lambda \tag{4.5}$$

Multiply through by $a^2\dot{a}$ and integrate,

$$2a\dot{a}\ddot{a} + \dot{a}^3 = \Lambda a^2\dot{a}$$

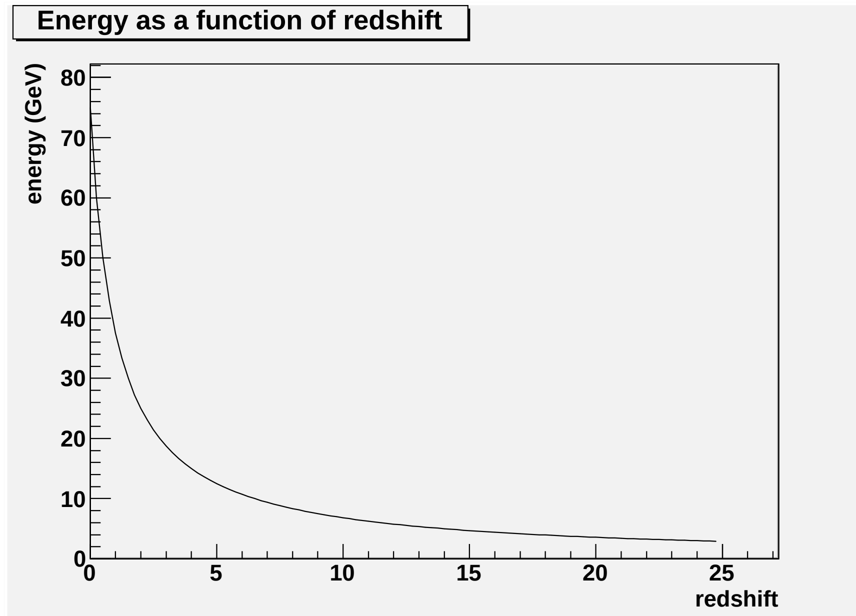

Figure 4.1: Energy versus redshift - The energy measured, $E(z)$, when receiving a photon that started out at $E_e = 75$ GeV, after it has been redshifted an amount z.

$$a\dot{a}^2 = \frac{\Lambda}{3}a^3 + K$$

where K is a constant of integration. Comparing this to the first Friedmann equation, we find that if we assume ρa^3 to be constant we can set K to be:

$$K = \frac{8\pi G\rho_0 a_0^3}{3}$$

Of course, we *don't* actually believe ρa^3 to be constant, but we do believe that our dark matter candidate should be stable over cosmological time scales. Therefore, the change in ρa^3 is assumed to be negligible.

If we do *not* assume a ρa^3 to be constant, we have for the first Friedmann equation multiplied by a^3:

$$\begin{aligned}
\dot{a}^2 a &= \frac{\Lambda}{3}a^3 + \frac{8}{3}\pi G\rho a^3 \\
&= \frac{\Lambda}{3}a^3 + \frac{8}{3}\pi G\left(\rho_{b0}(1+z)^3 + \rho_{DM0}(1+z)^3 e^{\frac{-(t-t_0)}{\tau_{\tilde{g}}}}\right)\frac{1}{(1+z)^3} \\
&= \frac{\Lambda}{3}a^3 + \frac{8}{3}\pi G\left(\rho_{b0} + \rho_{DM0}e^{\frac{-(t-t_0)}{\tau_{\tilde{g}}}}\right) \\
&= \frac{\Lambda}{3}a^3 + \frac{8}{3}\pi G\left\{\rho_{b0} + \rho_{DM0}\left[1 + \frac{(t_0-t)}{\tau_{\tilde{g}}} + \frac{(t_0-t)^2}{\tau_{\tilde{g}}^2 2!} + \cdots\right]\right\} \\
&= \frac{\Lambda}{3}a^3 + \frac{8}{3}\pi G\rho_c + \rho_{DM0}\sum_{i=1}^{\infty}\frac{(t_0-t)^i}{\tau_{\tilde{g}}^i i!}
\end{aligned}$$

If we let $\tau_{\tilde{g}} \to \infty$, we return to the expression we already found for the approximation of stable dark matter. Sadly, even if we limit ourselves to only including the first term of the sum as a correction to the stable DM expression, it does not look to be easily integrable. So we return to our approximation, which we will se *is* possible to solve analytically:

We want to integrate once more, and to this end we perform a substitution $a^3 = x^2$, which means that $(2/3)^2\dot{x}^2 = a\dot{a}^2$. We write our equation in its new and suggestive form:

$$\dot{x}^2 = \frac{3\Lambda}{2^2}x^2 + \left(\frac{3}{2}\right)^2 K$$

Now, $\frac{\mathrm{d}}{\mathrm{d}t}\sinh t = \cosh t$, and $\cosh^2 t = (\sinh^2 t + 1)$, so that's a promising start. Let's see what we can do with some mulitplicative constants.

$$x = A\sinh(Bt)$$

$$\dot{x} = AB\cosh(Bt)$$

$$\dot{x}^2 = (AB)^2\sinh^2(Bt) + (AB)^2$$

$$\dot{x}^2 = B^2x^2 + (AB)^2$$

So we get an equation for $a(t)$:

$$a^3 = \frac{3K}{\Lambda}\sinh^2\left(\frac{\sqrt{3\Lambda}t}{2}\right)$$

or

$$\frac{a}{a_0} = \left(\frac{\Omega_M}{\Omega_\Lambda}\right)^{1/3}\sinh^{2/3}\left(\frac{3H_0\Omega_\Lambda^{1/2}}{2}t\right)$$

So if we now use $a_0/a = 1 + z$ and shuffle this equation about for a bit, we get an expression for $t(z)$

$$t(z) = \frac{2}{3H_0\Omega_\Lambda^{1/2}} \sinh^{-1}\left[\left(\frac{\Omega_\Lambda}{\Omega_M}\right)^{1/2}(1+z)^{-3/2}\right]$$

This relation between time and redshift is what is visualized in figure 4.2. To save on writing in a bit, I define:

$$A = \frac{2}{3H_0\Omega_\Lambda^{1/2}}$$

$$B = \left(\frac{\Omega_\Lambda}{\Omega_M}\right)^{1/2}$$

Note that these are not equivalent to the multiplicative constants that showed up when we integrated $a\dot{a}^2$.

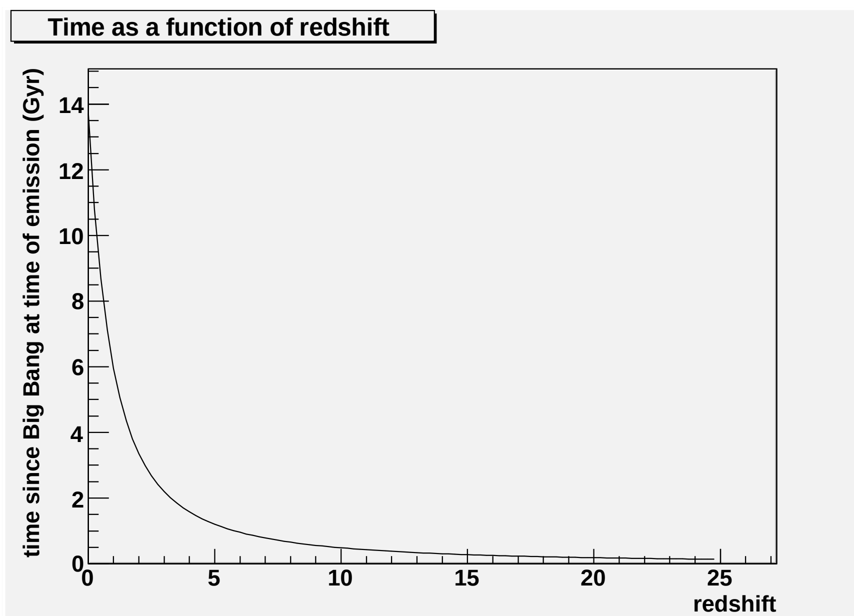

Figure 4.2: Time versus redshift - The time of emission of a photon received with a redshift z.

4.2.3 The Comoving Distance

To determine the comoving distance to an object, we start out with the Robertson-Walker metric with $k = 0$.

$$ds^2 = dt^2 - a^2(t)\left[dr^2 + r^2(d\theta^2 + \sin^2\theta d\phi^2)\right]$$

So a photon ($ds^2 = 0$) moving directly towards us ($d\theta = d\phi = 0$) gives

$$dt = a\ dr$$

Note that the speed at which light traverses the comoving coordinates is *not* constant. Rather, we have $dr/dt = 1/a$. Let's integrate this expression:

$$r(t_{em}) = \int_{t_{em}}^{t_0} \frac{dt'}{a(t')}$$

in terms of the time of emission, t_{em}. For added usefulness, let's parametrize r in terms of something observable, like the redshift. Differentiating redshift with respect to time, we get:

$$\begin{aligned} \frac{dz}{dt} &= -\frac{a_0}{a^2(t)}\frac{da}{dt} \\ -\frac{1}{a_0}\frac{a}{\dot{a}}dz &= \frac{dt}{a} \\ \frac{a}{\dot{a}} &= \frac{1}{H} \text{ (see eq. (4.2))} \end{aligned}$$

Then, when you integrate and adjust limits appropriately:

$$\frac{1}{a_0}\int_0^z \frac{dz'}{H(z')} = \int_{t_{em}}^{t_0} \frac{dt'}{a(t')} = r(z)$$

The minus sign disappears as the integral is "flipped" ($t' = t_0 \leftrightarrow z' = 0$). Luckily, we already have an expression for $H(z)$ to plug in

$$r(z) = \frac{1}{a_0 H_0}\int_0^z \frac{dz'}{\sqrt{(1+z)^3\left(\Omega_b + \Omega_{\tilde{g}} e^{\frac{-(t-t_0)}{\tau_{\tilde{g}}}}\right) + \Omega_\Lambda}} \tag{4.6}$$

Keeping in mind that $\sinh^{-1} x = \ln(x + \sqrt{x^2+1})$, the dark matter density in a comoving volume

$$\rho_{DM} = \rho_{DM0} e^{-\frac{t-t_0}{\tau_{\tilde{g}}}}$$

can now be expressed in terms of redshift instead of time. Now is the time to use the previously defined A and B. Along with $y = 1 + z$ it allows us to write:

$$\begin{aligned}
rho_z \rho_{DM} &= \rho_{DM0} e^{-\frac{t-t_0}{\tau_{\tilde{g}}}} \\
&= \rho_{DM0} \left\{ \frac{e^{t_0}}{e^{t(z)}} \right\}^{1/\tau_{\tilde{g}}} \\
&= \rho_{DM0} \left\{ \frac{e^{t_0}}{\exp\left[A \sinh^{-1}\left(By^{-3/2}\right)\right]} \right\}^{1/\tau_{\tilde{g}}} \\
&= \rho_{DM0} \frac{e^{t_0/\tau_{\tilde{g}}}}{\left\{\exp\left[\ln(By^{-3/2} + \sqrt{B^2 y^{-3} + 1})\right]\right\}^{A/\tau_{\tilde{g}}}} \\
&= \rho_{DM0} \frac{e^{t_0/\tau_{\tilde{g}}}}{\left\{B\left[y^{-3/2} + \sqrt{y^{-3} + (1/B^2)}\right]\right\}^{A/\tau_{\tilde{g}}}} \qquad (4.7)
\end{aligned}$$

This will be useful soon, but I'll keep using the exponential function in eq. (4.6) to save on writing.

We can now plot the relation between observed redshift and comoving coordinates, as well as the relation between distance and energy, by combining $r(z)$ and $E(z)$(Figures 4.3 and 4.4).

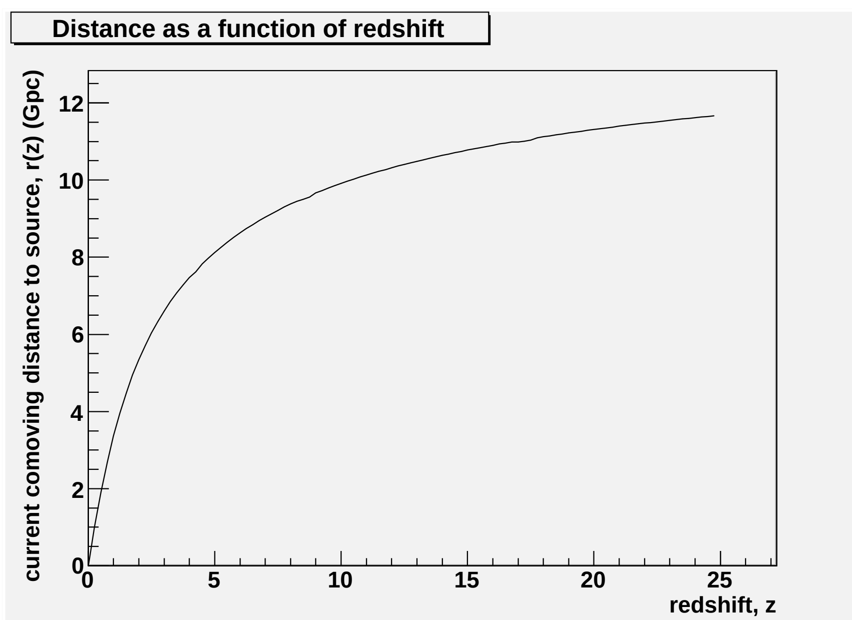

Figure 4.3: Radius versus redshift - The current comoving distance r to the place that sent out photons that are measured to be redshifted an amount z.

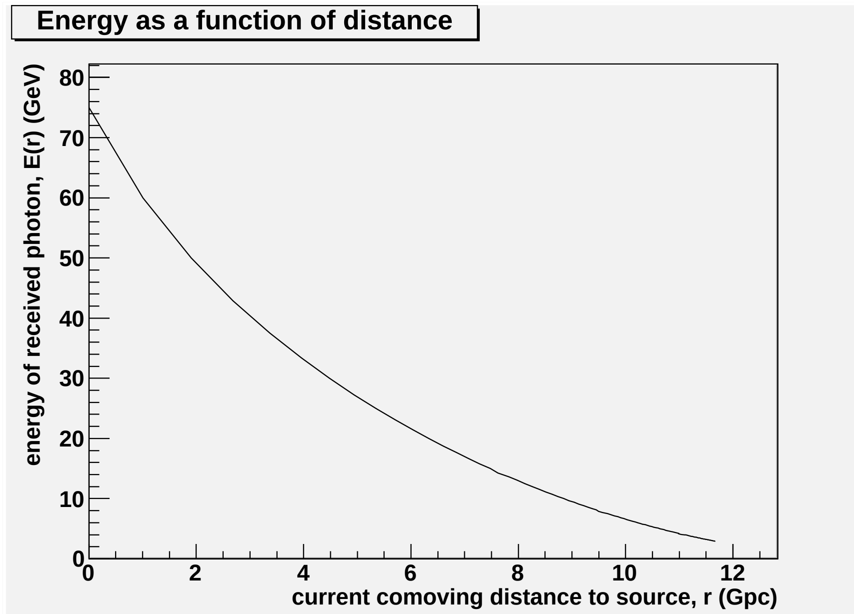

Figure 4.4: Energy versus distance - The current comoving distance $r(z)$ to the place a photon measured at $E(z)$ started out.

4.2.4 The cumulative flux from all distances.

In order find the cumulative flux from all distances, and arrive at the extragalactic contribution to our gamma readings, the expression $r(z)$ needs to be "tempered" with a constant C_γ similar to the one we had for the galactic contribution; in addition we want to account for the slight decay of gravitinos over cosmological timescales: First of all, the scaling factor at present, a_0, is unity by definition, so there's really no reason to keep it around. Secondly, it will be expedient to express the redshift as $y = 1 + z$. The effect of having the energy spread over a larger area at longer distances will, as before, necessitate the inclusion of a factor $1/4\pi$. The mean life of the gravitino, powers of E and the energy recorded enter in the same manner as last time, naturally. Finally, the factors expressing the number of particles in a comoving volume are now:

$$\frac{\rho_c \Omega_{\tilde{g}}}{m_{\tilde{g}}} \exp\left(\frac{t_0 - t(z)}{\tau_{\tilde{g}}}\right)$$

$$\Omega_{\tilde{g}} = \frac{\rho_{DM0}}{\rho_c}$$

So this is where we end up:

$$\left[E^2\frac{\mathrm{d}J}{\mathrm{d}E}\right]_{eg} = \frac{E^2}{m_{\tilde{g}}}C_\gamma\int_1^\infty \frac{\mathrm{d}N_\gamma}{\mathrm{d}(Ey)}\frac{\exp\left(\frac{t_0-t}{\tau_{\tilde{g}}}\right)y^{-3/2}}{\sqrt{\left[\Omega_b+\Omega_{\tilde{g}}\exp\left(\frac{t_0-t}{\tau_{\tilde{g}}}\right)\right]+y^{-3}\Omega_\Lambda}}\mathrm{d}y$$

$$C_\gamma = \frac{\Omega_{\tilde{g}}\rho_c}{4\pi\tau_{\tilde{g}}H_0}$$

I have simplified $t(z)=t$, to reduce the clutter.

The spectrum produced in the gravitino decay is now a little different. Well, the spectrum *produced* isn't actually different of course, but it looks different on our end. That is because energy received is a function of the redshift. If a photon is emitted at the time $t(z)$, at a distance $r(z)$, the energy we register is governed by eq. (4.4).

$$E = \frac{m_{\tilde{g}}}{2(1+z)}$$

That means we now have this expression for the energy yielded to us by a decay:

$$\frac{\mathrm{d}N_\gamma}{\mathrm{d}(Ey)} = \delta\left(Ey-\frac{m_{\tilde{g}}}{2}\right)$$

So we get energies ranging all the way from zero to $m_{\tilde{g}}/2$, with every energy corresponding to a specific redshift. Recall that the redshift is a measure of how much the universe has expanded since the photon was released. (Think of it as how much more space the wave is now stretched over, like a wavy line drawn on a rubber band.) That means it's a measure of how much time has passed since then, and ultimately therefore, the distance the photon has traveled. Let's now use $\delta(ax)=1/|a|\delta(x)$, and

$$\int_{-\infty}^{\infty}\delta(x)f(x)dx = f(0)$$

in the integral. The delta function "picks out" the single exact redshift and distance that yields a specific energy. We can evaluate the integral as a function of E, landing us:

$$\left[E^2\frac{\mathrm{d}J}{\mathrm{d}E}\right]_{eg} = \frac{E}{m_{\tilde{g}}}C_\gamma\frac{\exp\left(\frac{t_0-t}{\tau_{\tilde{g}}}\right)(m_{\tilde{g}}/2)^{-3/2}}{\sqrt{\left[\Omega_b+\Omega_{\tilde{g}}\exp\left(\frac{t_0-t}{\tau_{\tilde{g}}}\right)\right]E^{-3}+(m_{\tilde{g}}/2)^{-3}\Omega_\Lambda}}$$

We're almost ready. Now all we need is to take the Gaussian distribution of the actual measurement into account. Each "true" received value E_0 contributes a spectrum:

$$\left[E_0^2\frac{\mathrm{d}J}{\mathrm{d}E_0}(E)\right] = \frac{1}{\sqrt{2\pi}\sigma_0}\exp\left[\frac{(E-E_0)^2}{2\sigma_0^2}\right]\frac{E_0}{m_{\tilde{g}}}C_\gamma\frac{\exp\left(\frac{t_0-t}{\tau_{\tilde{g}}}\right)(m_{\tilde{g}}/2)^{-3/2}}{\sqrt{\left[\Omega_b+\Omega_{\tilde{g}}\exp\left(\frac{t_0-t}{\tau_{\tilde{g}}}\right)\right]E_0^{-3}+(m_{\tilde{g}}/2)^{-3}\Omega_\Lambda}} \tag{4.8}$$

Remember that the exponential function that shows up twice is also really a function of y, and needs to be evaluated at $y = m_{\tilde{g}}/2E_0$. Anyway, in order to get a theoretical value for the measured flux at some energy E, we need to sum all the expected contributions to the measurement from the surrounding values

$$f(E) = \int_{E_a}^{E_b} \left[E_i^2 \frac{\mathrm{d}J}{\mathrm{d}E_i}(E) \right] dE_i$$

with the limits set a suitable multiple of σ away from E_0 to ensure we get the whole contribution. If we did not include the exponential decay factor in the integral, assuming instead the comoving density to be constant, eq. (4.8) would have looked like this instead [28]:

$$\frac{1}{\sqrt{2\pi}\sigma_0} \exp\left[\frac{(E-E_0)^2}{2\sigma_0^2} \right] \frac{E_0}{m_{\tilde{g}}} C_\gamma' \frac{(m_{\tilde{g}}/2)^{-3/2}}{\sqrt{E_0^{-3} + (m_{\tilde{g}}/2)^{-3}\Omega_\Lambda/\Omega_M}}$$

$$C_\gamma' = \frac{\Omega_{\tilde{g}}\rho_c}{4\pi\tau_{\tilde{g}} H_0 \Omega_M^{1/2}}$$

Performing a numerical solution for these two possibilities give us the graphs of figure 4.5 to compare. As we can see from this figure, assuming a constant density in a comoving volume has no great impact on our results. This should come as no great surprise. Given that the mean life we're working with is some orders of magnitude larger than the age of the universe, it seems reasonable to assume that whatever has dissappeared should be negligible.

In anticipation of the next chapter we chang around the assumed mean life of our particle. We see that unless we change it greatly, the chief difference will be due to the inclusion of $\tau_{\tilde{g}}$ in C_γ. Halving $\tau_{\tilde{g}}$ will double the expected flux as is obvious in figure 4.6.

However, for large changes in tau, we will also se a move in the peak of the extragalactic contribution, as large redshift will correspond to earlier times with more dark matter. This effect is evident in figures 4.7 and 4.8.

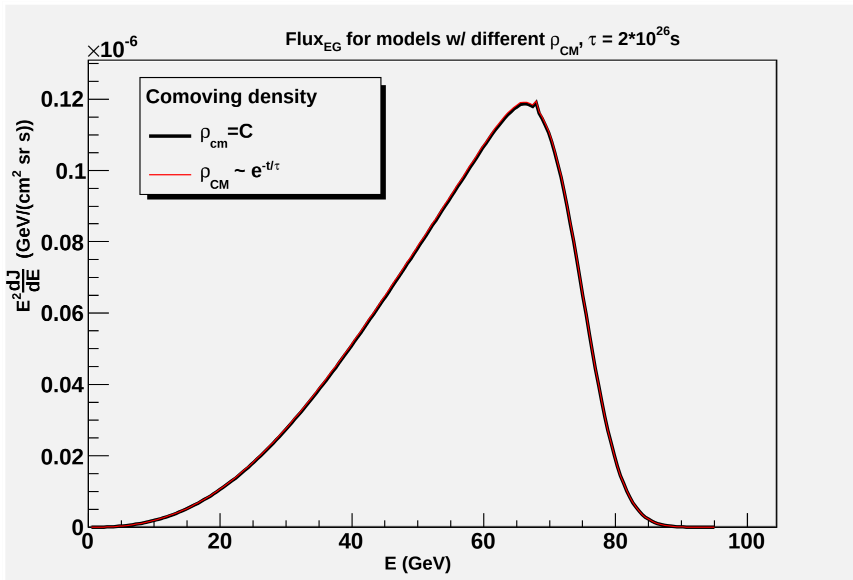

Figure 4.5: Normal vs quasi stable DM - A visualization of the effect on the expected contribution to the flux from gravitinos decaying outside the galaxy if we approximate by a constant comoving density.

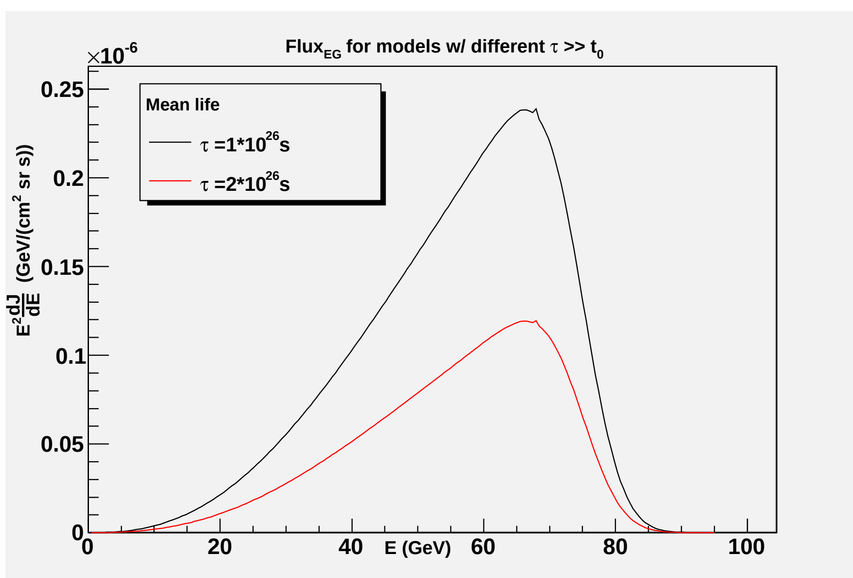

Figure 4.6: Difference in flux for a “small” difference in $\tau_{\tilde{g}}$. - A comparison of the expected contribution to the flux from gravitinos decaying outside the galaxy for different mean life times. The absolute values differ, but the shapes are similar.

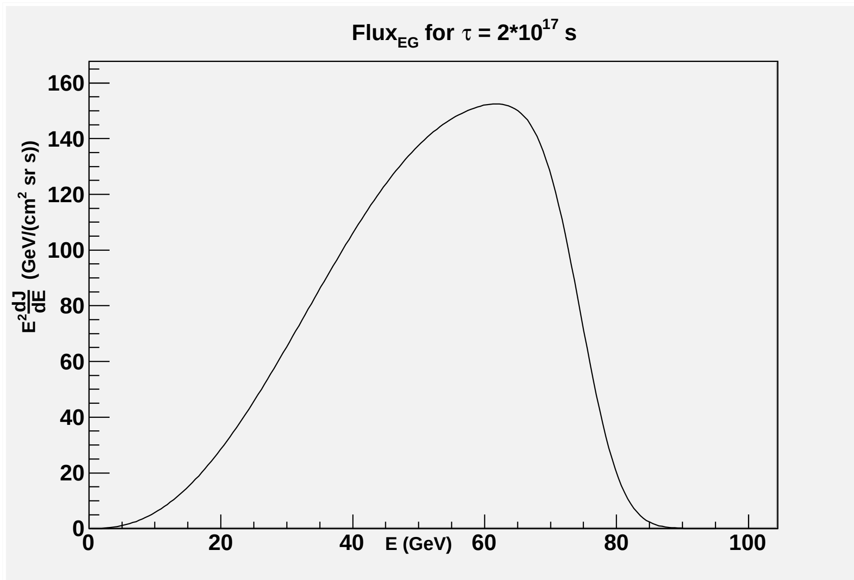

Figure 4.7: Flux for $\tau_{\tilde{g}} \sim 0.5 \times$ the age of the universe. - Expected extragalactic flux for a drastically different $\tau_{\tilde{g}}$. Note that the shape of the graph is starting to change.

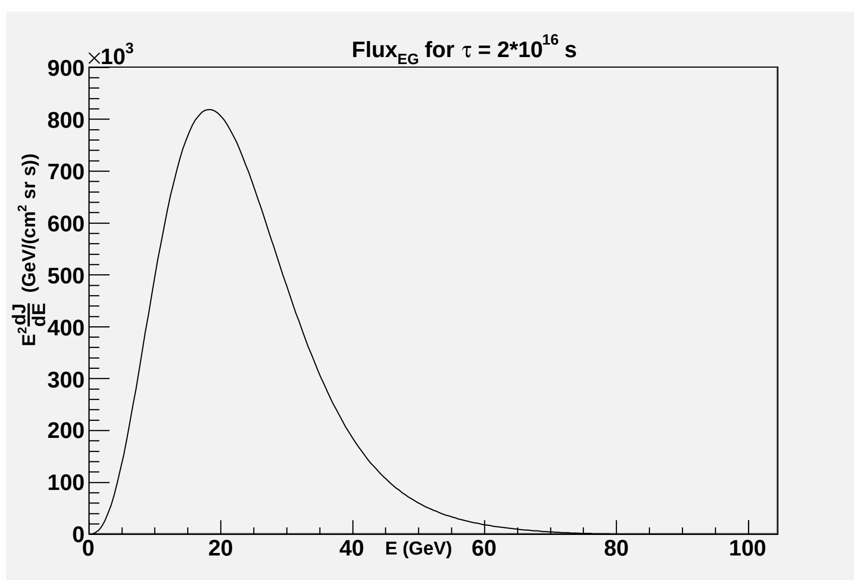

Figure 4.8: Flux for $\tau_{\tilde{g}} \sim 0.05 \times$ the age of the universe. - The expected extragalactic flux for a mean life that is 20 times smaller than t_0. The shape is now very different from that of figure 4.5.

Chapter 5

The sensitivity of EG-flux to changes in mean life

5.1 Why investigate this behavior?

The reason we want to see what happens with the extragalactic flux when we vary $\tau_{\tilde{g}}$ is this: As $\tau_{\tilde{g}}$ *decreases* the difference in dark matter density over cosmological timescales *increases*. Is it possible to find a mean life such that there is a noticeable change in the shape of our expected signal?

For the values used as our starting point, based on those of Ibarra/Tran [28], the extragalactic flux is merely an unfocused little brother of the galactic one. It's about a factor 5 smaller, with the peak at roughly the same spot, and with a larger spread. We're looking for a mean life such that the two peaks separate. At some point, the change in $\tau_{\tilde{g}}$ means that the increased presence of dark matter in aeons gone by will mean that the extragalactic flux actually dominates.

5.2 Considerations when changing the mean life

Of course, normally you can not play around with the mean life of a particle completely at will. A number of factors come into play. First of all, the mean life of a particle is usually not ours to decide at all. It is set, and no amount of wishful thinking can change it. Luckily, when we are looking for particles that may or may not exist, we have some leeway.

By its very nature, the properties of such an elusive particle are not completely decided. For if they were, it would be because we had found some way of confirming them, thereby confirming the very existence of the particle that is supposed to be in doubt. Very well then, we will decide that our particle should have the sort of properties we need it to.

Alas, it is not so simple. To look for every possible particle that could come out every possible theory would be counterproductive (and tedious). We have to limit ourselves to theories that are internally consistent, and produce results that we have the ability to check.

So in our case that means, primarily, that there must be some set of values for the (admittedly many) SUSY parameters that produces a particle that behaves like we want it to. And that also allows the rest of the universe to keep in business. This is a task that started out as being cleverly outsourced. But now that I am changing things around, it is beyond optimistic to think that I should be able to simply assume all other properties to be conserved.

Next, the notion of more or less constant dark matter density over the ages is nothing to sneeze at. Close to the beginning of this whole thesis, I mentioned that dark matter plays a vital part in the formation of structure in the early universe. This to the extent that the differences in simulated development of structure with and without dark matter is regarded as one of the important justifications that we're looking for the stuff. It stands to reason that before proposing a seriously unstable dark matter particle, you should maybe check if everything will still be all right with the universe.

There are purely practical difficulties as well. When dealing with general relativity in a previous chapter, I had to assume a pressureless universe to get a nice and analytical expression for time as a function of redshift. It seems I jumped the gun a bit there, as the radiation released from more eagerly decaying dark matter could certainly play havoc with that assumption. Not only that, I even had to assume a *constant comoving matter density* to get that time versus redshift graph, and that certainly breaks down sooner than we'd like.

Examining all of these issues, and figuring out to what degree there is a way around them, could take quite some time. Luckily, there is another little detail that allows us to get some answers by playing 'what if'. Let's say I did manage to figure out all of the above. Let's say I didn't. Is there still some information to be gleaned from what we already know? It turns out there is.

5.3 The effect of altering mean life

On the following pages I have collected many figures showing the expected extragalactic flux for a wide variety of values for $\tau_{\tilde{g}}$. Some of them are repeated from the earlier chapter, simply for completeness' sake. They start at the value used at the very beginning ($2 \cdot 10^{26}$ s) being compared directly to the one we get if the mean life is only half as big. It then makes a big jump to $\tau_{\tilde{g}} = 4 \cdot 10^{17}$ s, before settling on a more even spread.

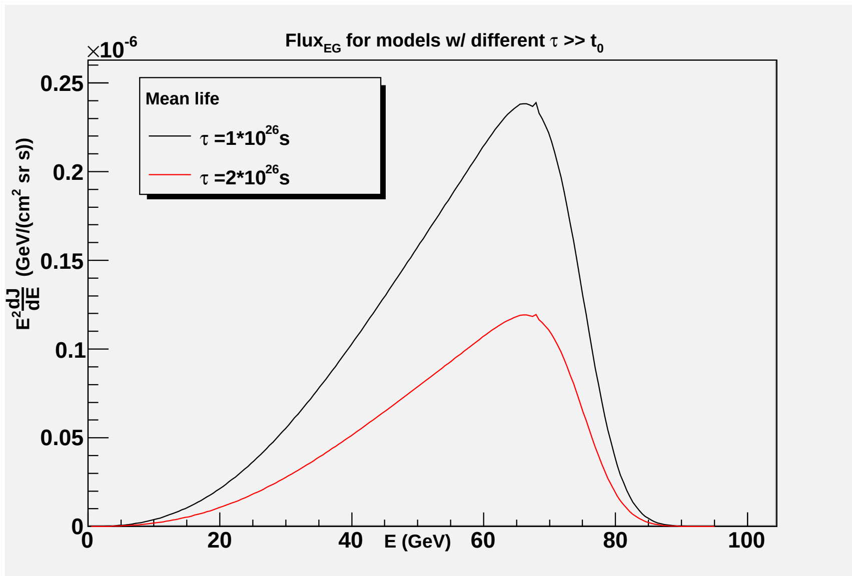

Figure 5.1: Difference in flux for a "small" difference in $\tau_{\tilde{g}}$. - A comparison of the expected contribution to the flux from gravitinos decaying outside the galaxy for different mean life times. The absolute values differ, but the shapes are similar.

Already after these three first figures (5.1, 5.2, and 5.3), we learn something. Even for a massively changed mean life, the shape of the graph, and the placing of its peak, remains the same. The reason is this: The absolutely greatest value possible in the argument of the exponential function controlling the decay is t_0:

$$\rho(t) = \rho_{DM0} * e^{\frac{-(t-t_0)}{\tau_{\tilde{g}}}}$$

This means that:

$$\tau_{\tilde{g}} \gg t_0 \Rightarrow \rho(t) \simeq \text{constant}$$

As long as we stay in this area, the sole effect of multiplying $\tau_{\tilde{g}}$ by some factor, is multiplying the expected flux by the inverse of the same factor. So if we mulitply by 10^{-6}, all that happens is that the peaks of our graphs are a million times higher, but we still can't tell them apart. The assumptions made during the general relativity chapter still hold up, but that's it for the good news.

As we know by know, these figures have can't really tell us too much, as we're moving further and further into the territory where we can not trust $t(z)$, but let's have a look:

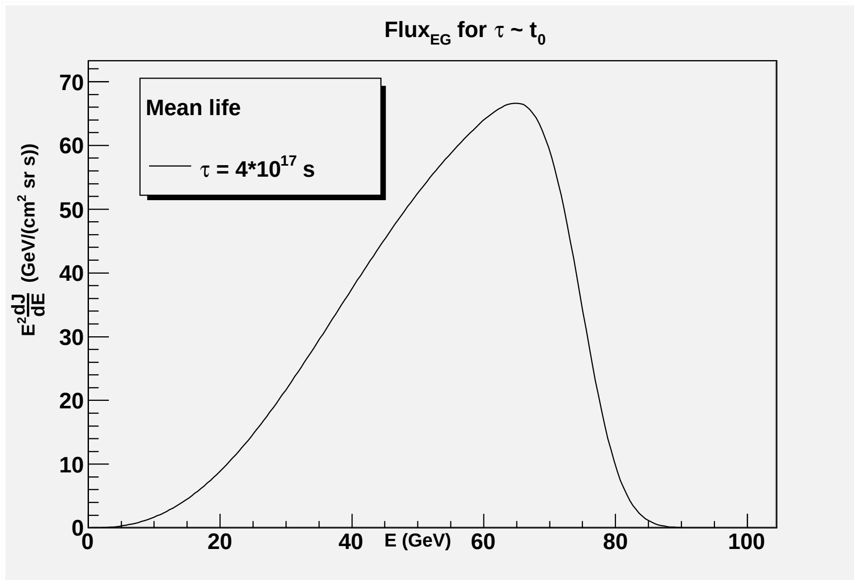

Figure 5.2: Flux for $\tau_{\tilde{g}} \sim$ the age of the universe. - At this point, the graph is still no different in its basic shape.

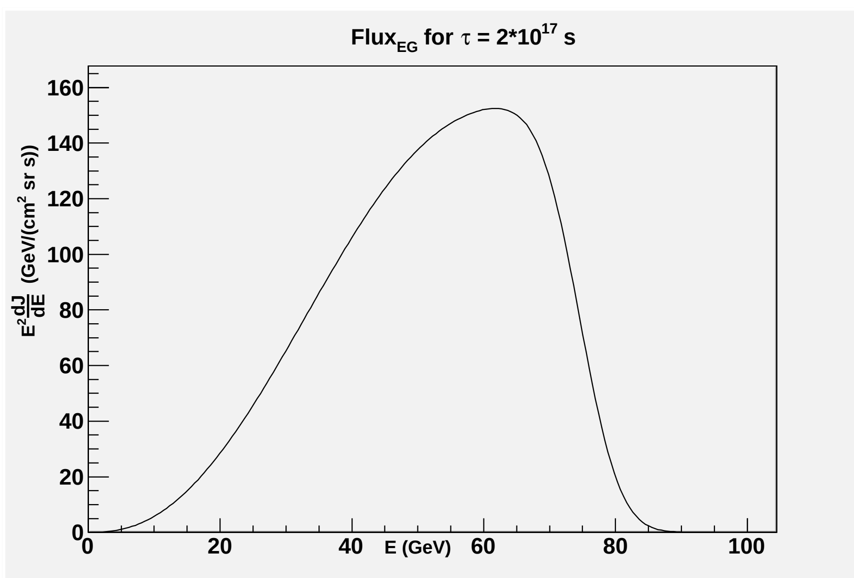

Figure 5.3: Flux for $\tau_{\tilde{g}} \sim 0.5 \times$ the age of the universe. - Expected extragalactic flux for a drastically different $\tau_{\tilde{g}}$. Note that the shape of the graph is starting to change.

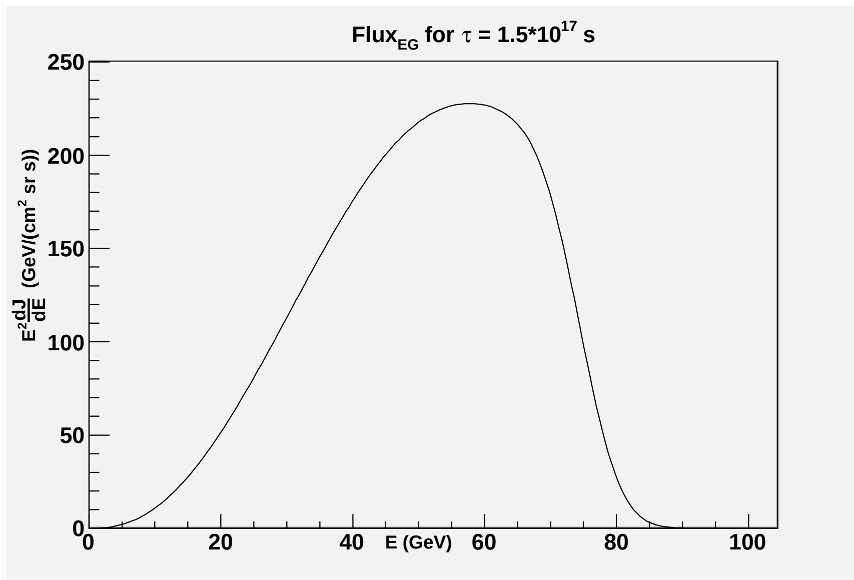

Figure 5.4: $\tau_{\tilde{g}} = 1.5 \cdot 10^{17}$ **s** - This and the following figures show the development of the peak position as $\tau_{\tilde{g}}$ decreases.

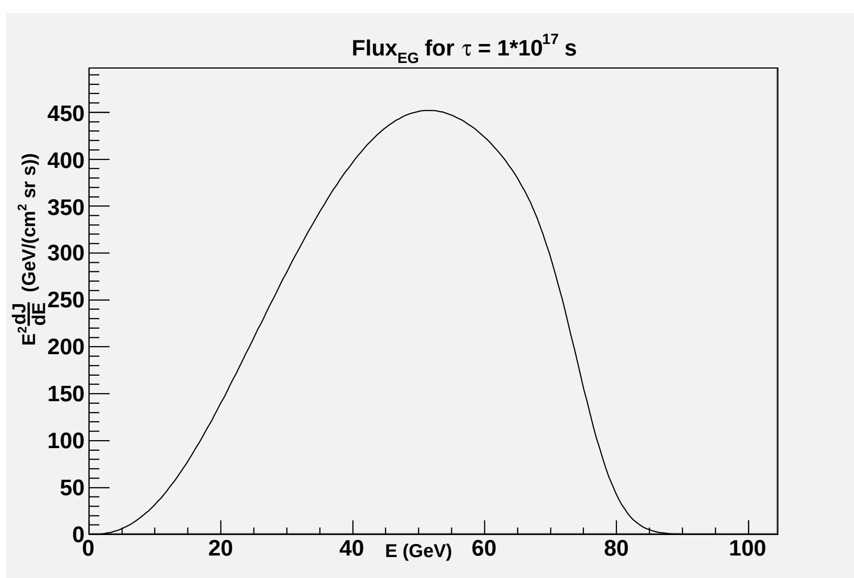

Figure 5.5: $\tau_{\tilde{g}} = 1 \cdot 10^{17}$ **s** -

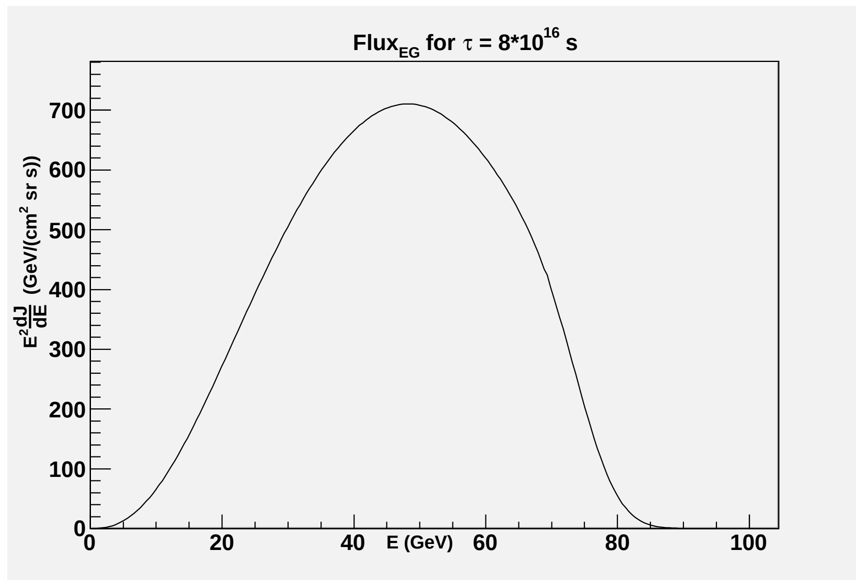

Figure 5.6: $\tau_{\tilde{g}} = 8 \cdot 10^{16}$ **s -**

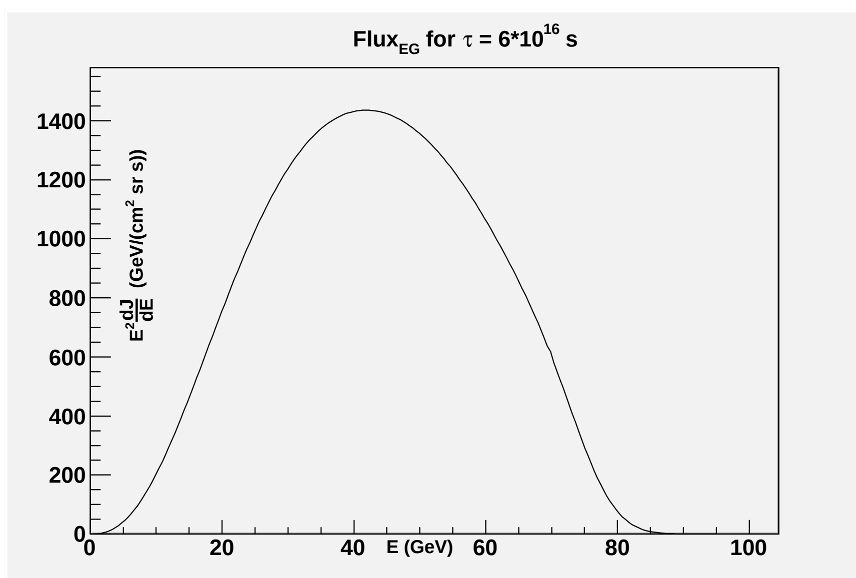

Figure 5.7: $\tau_{\tilde{g}} = 6 \cdot 10^{16}$ **s -**

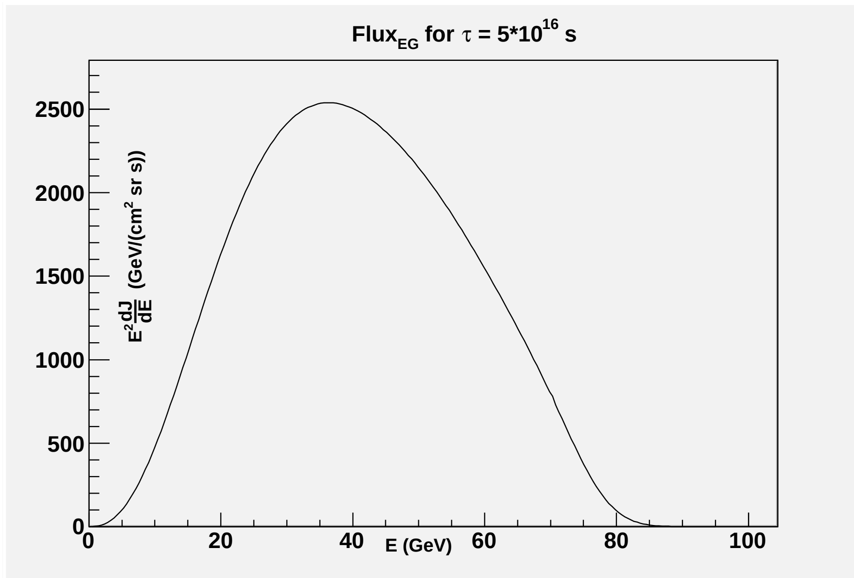

Figure 5.8: $\tau_{\tilde{g}} = 5 \cdot 10^{16}$ s -

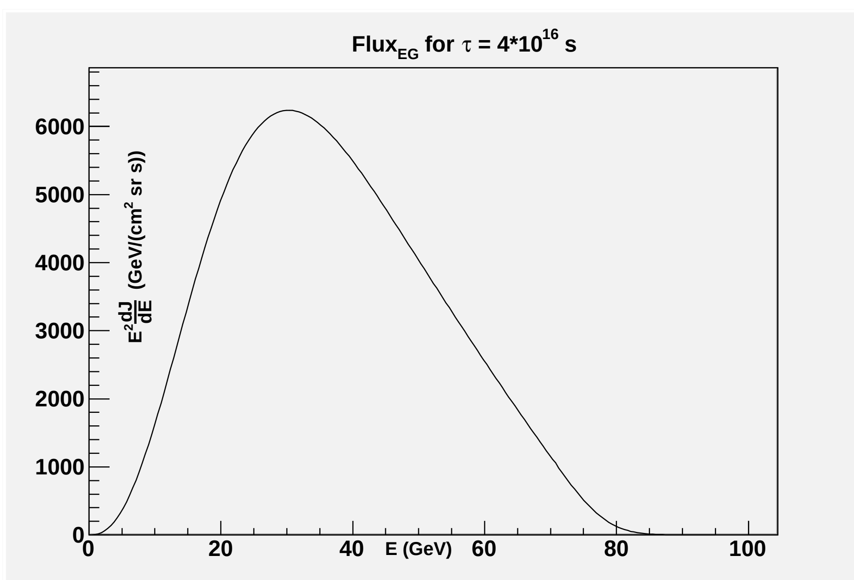

Figure 5.9: $\tau_{\tilde{g}} = 4 \cdot 10^{16}$ s -

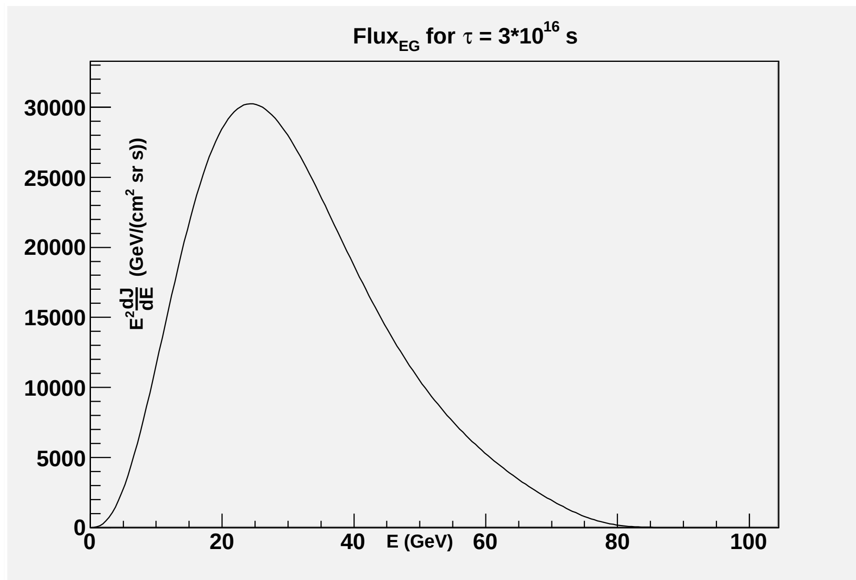

Figure 5.10: $\tau_{\tilde{g}} = 3 \cdot 10^{16}$ **s -**

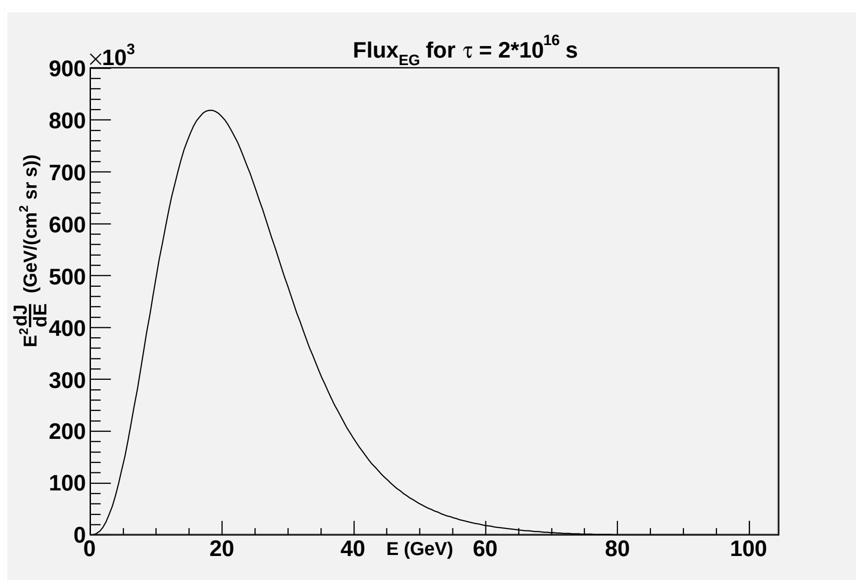

Figure 5.11: $\tau_{\tilde{g}} = 2 \cdot 10^{16}$ **s -**

The peak is moving progressively further to the left, as we expected. This represents the higher dark matter density of the past sending us higher intensities of radiation, albeit with each individual photon carrying less energy. Let's examine the movement of the peak a bit more:

We could try to find the derivative of the flux with respect to E, set it to zero, and plot the resulting points as a function of $\tau_{\tilde{g}}$, but we soon run into difficulties. The integral in Eq. (4.8) is not over E, and so we move a partial derivative operator into the integrand. However, the result no more invites analytical solutions than did it's predecessor. Trying to numerically solve a derivative consisting of infinitesimal pieces hovering around zero, gives predictably disastrous results, as many books deal with, see for instance [43]. Books like these do list tricks to handle these things, but it is so much easier to simply pick out the top values from the flux graphs already computed and plot them as a function of the mean life (figure 5.12):

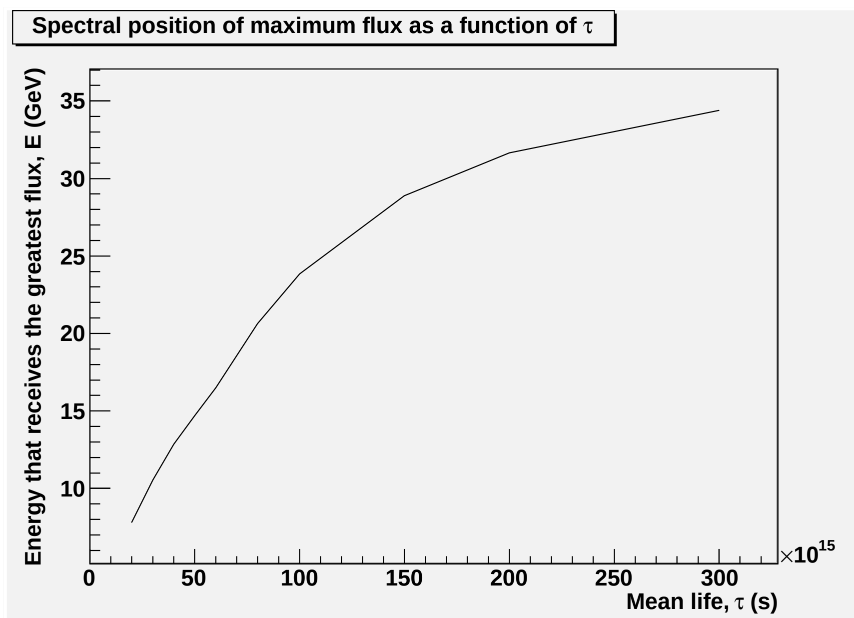

Figure 5.12: Energy peak position for different decay rates - This plot shows the photon energy where a model with a mean life $\tau_{\tilde{g}}$ expects the highest intensity.

We see that for differences at high $\tau_{\tilde{g}}$, the position of the peak changes slowly, as noted when I commented on the three first figures. For smaller $\tau_{\tilde{g}}$, things speed up, but there is less reason to be confident about the values in this area.

Exactly when and to what degree our reasoning breaks down, is of less importance than one might think, however. We have already established that by varying the mean life considerably in the region where we can approximate ρ_{DM} to be constant, we can deduce that the shape stays similar. All the while the intensity of the flux goes above the values measured by EGRET by some orders of magnitude. What's more, in this region of $\rho(z) \simeq C$, the galactic and extragalactic component depen upon $\tau_{\tilde{g}}$ in the same manner. We will definitely not be able to tell them apart by changing the mean life.

As a final thought, there is always the possibility that if you deal with a particle that does not decay directly to a photon and a neutrino, the ultimate product may be a collection of photons with less intensity. These could then line up with measurement for a different interval of tau. But you would still face the problems that tag along when a comoving density varies with time, and you would lose the characteristic monochromatic peak for the local flux. The already diffuse nature of the extragalactic signal would not be helped by this.

Chapter 6

Conclusion

I set out to study the effect of adjusting the mean life of slowly decaying gravitinos on the extragalactic flux component. We have seen that choice of model for dark matter distribution in the milky way has ultimately little effect on the feasibility of this goal, as the effect on signal amplitude of reasonable models does not compare with that of mean life adjustment. We discovered that there is a great effect on the extragalactic and galactic overall flux intensity of adjusting the mean life. It has been shown that the intensity vastly exceeds the values permitted by measurement, long before the goal of a discernible change in overall signal shape has been reached. This because the staring point for τ, which give values that conform to measurement, dwarfs the age of the universe by several orders of magnitude. Therefore, the peak position of the spectrum is resilient to change, while the peak value is not. We have also demonstrated that ensuring the viability of our chosen models in the region of shape change is not a trivial task, as the well behaved nature of the time-redshif relation depends on a dominance of stable matter.

There is the possibility of getting a different result with particles that decay differently, but this venture also faces difficulties.

Appendix A

Constants

present day Hubble expansion rate	H_0	$100h$ km s^{-1} Mpc^{-1}
present day normalized Hubble expansion rate	h	0.73(3)
Critical density of the Universe	ρ	$1.053 \cdot 10^{-5} h^2$ GeV/cm^3
pressureless matter density of the Universe	$\Omega_M = \rho_M/\rho_c$	0.24
baryon density of the Universe	$\Omega_b = \rho_b/\rho_c$	0.0425
dark matter density of the Universe	$\Omega_{\rm dm} = \Omega_m - \Omega_b$	0.20
dark energy density of the Universe	Ω_Λ	0.73(3)
speed of light	c	$2.9979 \cdot 10^8$ m s^{-1}
parsec	pc	$3.0857 \cdot 10^{16}$ m
Newtonian gravitational constant	G_N	$6.6743(7) \cdot 10^{-11}$ m^{3}kg^{-1}s^2

Appendix B

The Components of Einstein's Equations

In this appendix, various components needed to arrive at the Friedmann equations are listed.

Christoffel Symbols:

$$
\begin{aligned}
\Gamma^0_{11} &= (\frac{a\dot{a}}{1-kr^2} \\
\Gamma^0_{22} &= r^2 a\dot{a} \\
\Gamma^0_{33} &= r^2 a\dot{a}\sin^2\theta \\
\Gamma^1_{01} &= \Gamma^1_{10} = \frac{\dot{a}}{a} \\
\Gamma^1_{11} &= \frac{kr}{1-kr^2} \\
\Gamma^1_{22} &= r(kr^2-1) \\
\Gamma^1_{33} &= r(kr^2-1)\sin^2\theta \\
\Gamma^2_{02} &= \Gamma^2_{20} = \frac{\dot{a}}{a} \\
\Gamma^2_{12} &= \Gamma^2_{21} = \frac{1}{r} \\
\Gamma^2_{33} &= -\sin\theta\cos\theta \\
\Gamma^3_{03} &= \Gamma^3_{30} = \frac{\dot{a}}{a} \\
\Gamma^3_{13} &= \Gamma^3_{31} = \frac{1}{r} \\
\Gamma^3_{23} &= \Gamma^3_{32} = \cot\theta
\end{aligned}
\tag{B.1}
$$

components of the Riemann curvature tensor:

$$R^0_{101} = \frac{a\ddot{a}}{1-kr^2}$$

$$\begin{aligned}
R^0_{202} &= r^2 a\ddot{a} \\
R^0_{303} &= r^2 a\ddot{a}\sin^2\theta \\
R^1_{001} &= \frac{\ddot{a}}{a} \\
R^1_{212} &= r^2(\dot{a}^2+k) \\
R^1_{313} &= r^2(\dot{a}^2+k)\sin^2\theta \\
R^2_{002} &= \frac{\ddot{a}}{a} \\
R^2_{112} &= -\frac{(\dot{a}^2+k)}{1-kr^2} \\
R^2_{323} &= r^2(\dot{a}^2+k)\sin^2\theta \\
R^3_{003} &= \frac{\ddot{a}}{a} \\
R^3_{113} &= -\frac{(\dot{a}^2+k)}{1-kr^2} \\
R^3_{223} &= -r^2(\dot{a}^2+k)
\end{aligned} \tag{B.2}$$

References

[1] E. M. Henley and A. Garcia. *Subatomic Physics*. World Scientific Publishing, 2007. 1

[2] F. Mandl and B. Shaw. *Quantum Field Theory*. John Wiley & Sons, 1993. 1, 9, 16

[3] C. Kiefer. **Quantum Gravity: General Introduction and Recent Developments.** *Annalen Phys.*, **15**:129–148, 2005. 1

[4] S. P. Martin. **A Supersymmetry Primer**. arXiv:hep-ph/9709356v5, 2008. 2

[5] F. Zwicky. **Die Rotverschiebung von Extragalaktischen Nebeln**. *Helv. Phys. Acta.* , **6**:110, 1933. 2

[6] D. Hooper. **TASI 2008 Lectures on Dark Matter**. arXiv:hep-ph/0901.4090v1, 2009. 2, 7, 8

[7] F. Zwicky. **On the Masses of Nebulae and of Clusters of Nebulae**. *The Astrophysical Journal*, **86**:217, 1937. 3

[8] S. van den Bergh. **The Early History of Dark Matter**. *The Publications of the Astronomical Society of the Pacific*, **111**:657, 1999. 3

[9] C. Amsler et al. **Review of Particle Physics**. *Physics Letters*, **B 667**, 2008. 3

[10] M. Milgrom. **A modification of the Newtonian dynamics as a possible alternative to the hidden mass hypothesis**. *The Astrophysical Journal*, **270**:365–370, 1983. 3, 6

[11] V. C. Rubin and W. K. Ford Jr. **Rotation of the Andromeda Nebula From a Spectroscopic Survey of Emission Regions**. *The Astrophysical Journal*, **159**:379, 1970. 3

[12] V. C. Rubin et al. **Rotation veklocities and a Comparison of Sa, Sb and Sc Rotation Properties**. *The Astrophysical Journal*, **289**:81, 1985. 3

[13] Phil Hibbs, 2005. Wikimedia commons under Creative Commons Attribution-Share Alike license. 4

[14] A. Einstein. **Lens-Like Action of a Star by the Deviation of Light in a Gravitational Field**. *Science*, **84**:506, 1936. 4

[15] S. W. Allen. **Resolving the discrepancy between X-ray and gravitational lensing mass measurements for clusters of galaxies**. *Monthly Notices of the Royal Astronomical Society*, **296**:392–406, 1997. 4

[16] T. Kitching R. Massey and J. Richard. **The Dark Matter of Gravitational Lensing**. arXiv:astro-ph.CO/1001.1739v2, 2010. 4

[17] D. Clowe et al. **A Direct Empirical Proof of the Existence of Dark Matter**. *The Astrophysical Journal*, **648**, 2006. 5

[18] V. Springel, C. S. Frenk, and S. D. M. White. **The large-scale structure of the Universe**. *Nature*, **440**:1137, 2006. 5

[19] M. Milgrom. **A Modification of the Newtonian Dynamics: Implications for Galaxies**. *The Astrophysical Journal*, **270**:371–383, 1983. 6

[20] R. H. Sanders. **Modified gravity without dark matter**. *Lecture Notes in Physics*, **720**:375–402, 2006. 6

[21] S. S. McGaugh. **A Novel Test of the Modified Newtonian Dynamics with Gas Rich Galaxies**. *Physical Review Letters*, **106**, 2001. 7

[22] N. F. Bell, J. B. Dent, A. J. Galea, T. D. Jaques, L. M. Krauss, and T. J. Weiler. **W/Z Bremsstrahlung as the Dominant Annihilation Channel for Dark Matter, Revisited**. arXiv:hep-ph/1104.3823v1, 2011. 7

[23] G. Bertone, D. Hooper, and J. Silk. **Particle dark matter: evidence, candidates and constraints**. *Physics Reports*, **405**:279–390, 2005. 8

[24] M. Lovell, V. Eke, C. Frenk, L. Gao, A. Jenkins, T. Theuns, J. Wang, A. Boyarsky, and O. Ruchayskiy. **The Haloes of Bright Satellite Galaxies in a Warm Dark Matter Universe**. arXiv:astro-ph/1104.2929v1, 2011. 8

[25] D. J. Griffiths. *Introduction to Electrodynamics*. Prentice-Hall International, Inc., 1999. 16

[26] I. J. R. Aitchison and A. J. G. Hey. *Gauge Theories in Particle Physics*. Taylor & Francis, 2002. 16, 17

[27] I. J. R. Aitchison. *Supersymmetry in Particle Physics: An Elementary Introduction*. Cambridge University Press, 2007. 17

[28] A. Ibarra and D. Tran. **Gamma-Ray Spectrum from Gravitino Dark Matter Decay**. *Phys. Rev. Lett.*, **100**, 2008. 17, 20, 23, 25, 45, 49

[29] A. W. Strong, I. V. Moskalenko, and O. Reimer. **A New Determination of the Extragalactic Diffuse Gamma-Ray Background from EGRET Data**. *The Astrophysical Journal*, **613**:956, 2004. 20

[30] K. H. Kampert et al. **Recent Results from Kascade-Grande**. arXiv:astro-ph/0608340v1, 2006. 22

[31] J. B. Hartle. *Gravity: An Introduction to Einstein's General Relativity*. Pearson Education, 2003. 22, 31

[32] V. Springel et al. **Simulations of the formation, evolution and clustering of galaxies and quasars**. *Nature*, **435**:629–636, 2005. 23

[33] J. F. Navarro, C. S. Frenk, and S. D. M. White. **The Structure of CDM Halos**. *The Astrophysical Journal*, **462**:563–575, 1996. 23

[34] D. Merritt, A. W. Graham, B. Moore, J. Diemand, and B. Tersić. **Empirical Models for Dark Matter Halos. I. Nonparametric Construction of Density Profiles and Comparison with Parametric Models**. *The Astronomical Journal*, **132**:2685–2700, 2006. 23

[35] A. D. Ludlow, J. F. Navarro, M. Boylan-Kolchin, V. Springel, A. Jenkins, C. S. Frenk, and S. D. M. White. **The Density and Pseudo-Phase-Space Density Profiles of CDM halos**. arXiv:astro-ph.CO/1102.0002v1, 2011. 23

[36] J. F. Navarro, E. Hayashi, C. Power, A. Jenkins, C. S. Frenk, et al. **The inner structure of ΛCDM haloes - III. Universality and asymptotic slopes**. *Monthly Notices of the Royal Astronomical Society*, **349**:1039, 2004. 23

[37] L. Hernquist. **An analytical model for spherical galaxies and bulges**. *Astrophysical Journal*, **356**:359–364, 1990. 28

[38] P. Prugniel and F. Simien. **The fundamental plane of early-type galaxies: non-homology of the spatial structure.** *Astronomy and Astrophysics*, **321**:111–122, 1997. 29

[39] L. Bergström and A. Goobar. *Cosmology and Particle Astrophysics*. Praxis Publishing, 2004. 32

[40] P. J. E. Peebles. *Principles of Physical Cosmology*. Princeton University Press, 1993. 34, 36

[41] Ø. Grøn. **A new standard model of the universe**. *European Journal of Physics*, **23**:135–144, 2002. 37

[42] A. Macdonald. **Comment on "The Cosmic Time in Terms of the Redshift", by Carmeli et al**. *Foundations of Physics Letters*, **19**:631–632, 2006. 37

[43] C. F. Gerald and P. O. Wheatley. *Applied Numerical Analysis*. Pearson Education, Inc., 2004. 57